SYNTHETIC DELIVERY SYSTEMS THAT CONTROL RELEASE OF ANTICANCER AGENTS FROM EARLY ENDOSOMES

By

Ning Yang

Submitted to the graduate degree program in Medicinal Chemistry and the Graduate Faculty of the University of Kansas in partial fulfillment of the requirements for the degree of Master of Science.

_____

Chairperson Dr. Blake R. Peterson

_____

Dr. Michael Rafferty

_____

Dr. Paul R. Hanson

Date Defended: September 6, 2013

The Thesis Committee for Ning Yang

certifies that this is the approved version of the following thesis:

SYNTHETIC DELIVERY SYSTEMS THAT CONTROL RELEASE OF ANTICANCER AGENTS FROM EARLY ENDOSOMES

_____

Chairperson Dr. Blake R. Peterson

Date approved: September 6, 2013

ABSTRACT

Tubulin-binding agents are an important class of therapeutics for cancer chemotherapy. However, their application can be limited by systemic toxicity, poor tissue specificity, and drug resistance. To address these issues, modification of tubulin-binding agents with drug delivery systems has shown significant promise. Our group has developed a novel technology for delivery of small molecules and macromolecules into mammalian cells. By mimicking small natural cell surface receptors, cargo linked to the membrane anchor *N*-alkyl-3β-cholesterylamine can be internalized through a clathrin-mediated endocytic pathway and trapped in early/recycling endosomes. Co-administration with endosome-disruptive peptides enable 3β-cholesterylamine-conjugated cargo to escape these early/recycling endosomes of living mammalian cells. This approach can be highly efficient as evidenced by fluorescence-based assays. To explore the potential of this system for delivery of tubulin-binding agents, we designed and synthesized a series of colchicine- and colchinol methyl ether-cholesterylamine conjugates. These disulfide-linked compounds were designed to deliver tubulin-binding agents into early/recycling endosomes to minimize their cytotoxic effect. Only upon the activation by an endosome disruptive peptide would these conjugates be released into the cytosol. Cleavage of a disulfide bond in a linker region by glutathione provides a mechanism of release. Cell viability assays demonstrated that carefully-designed conjugates to cholesterylamine can substantially reduce the toxicity of tubulin-binding agents by trapping the warhead in endosomes. After activation by endosome disruptive peptides, conjugates with a glutamic acid residue in the linker region proximal to colchinol methyl ether showed high potency against several cancer cell lines including Jurkat lymphocytes (T-cell leukemia) and PC3 prostate cancer cells.

ACKNOWLEDGEMENTS

First of all, I thank my advisor, Dr. Blake Peterson for guidance, patience, and support over the past years. I would like to show sincere gratitude to my thesis committee members, Dr. Michael Rafferty, and Dr. Paul R. Hanson, for their precious time and invaluable opinions.

I also would like to thank individuals that have supported the work described in this thesis. Thanks to the Peterson lab members past and present, specifically Dr. Chamani Perera, Dr. Ze Li, and Mr. David Hymel.

Funding for this work was provided by the National Institutes of Health (R01-CA83831) and the University of Kansas Cancer Center.

TABLE OF CONTENTS

LIST OF FIGURES

LIST OF TABLES

Chapter 1. Tubulin-Binding Agents in Cancer Chemotherapy

1.1 Introduction

Microtubules are components of the cytoskeleton with important roles in a variety of cellular functions including intracellular transport, maintenance of cell shape, polarity, cell signaling, and mitosis.[1] During mitosis, microtubules form the mitotic spindle that transports daughter chromosomes to separate poles of the dividing cell. Microtubules are noncovalent polymers of α- and β-tubulin heterodimers assembled in a filamentous tube-shaped structure. Consequently, tubulin-binding agents are widely used in cancer chemotherapy due to the important role of microtubules in cell division.[2] Their efficacy has been demonstrated in the clinic for the treatment of a wide variety of human cancers, including breast, lung, ovarian, and prostate, as well as haematological malignancies and childhood cancers.[3]

Tubulin-binding agents are known to interact with tubulin at four binding sites: the laulimalide, taxane/epothilone, vinca alkaloid, and colchicine sites (Figure 1.1). Similar to paclitaxel, laulimalide can promote the tubulin-microtubule assembly, but binds to a different site on microtubules (Figure 1.2).[4] Taxanes, including docetaxel and paclitaxel, bind to polymerized microtubules at the inner surface of the β subunit (Figure 1.2), and are widely used in the treatment of lung, breast, ovarian and bladder cancers. Taxanes promote tubulin stabilization, thereby interfering with tubulin dynamics.[5] Vinca alkaloids generally bind with high affinity to one or a few tubulin molecules at the tip of microtubules and promote depolymerization of microtubules. (Figure 1.2).[6] The fourth group of microtubule interfering agents is represented by colchicine, which also induces microtubule depolymerization of microtubules (Figure 1.2).[6]

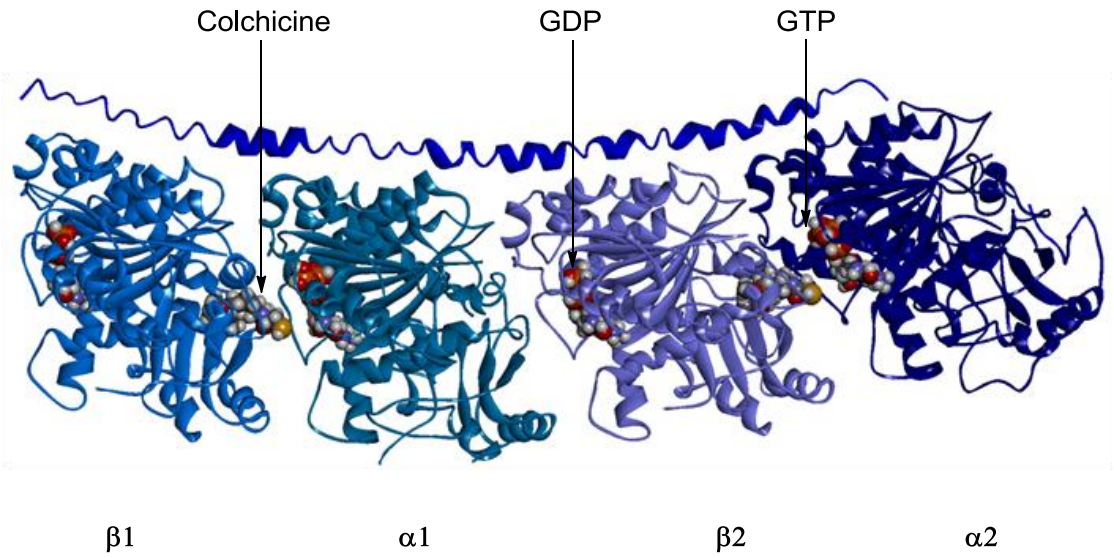

Figure **1.1**: X-ray structure of colchicine-β tubulin binding complex (PDB code: 1SA0).

In contrast to agents that bind to the other three sites, colchicine binds with high affinity to tubulin and is copolymerized into microtubules. Colchicine binding to β-tubulin results in a curved tubulin dimer. This prevents the formation of a straight structure, due to a steric clash between colchicine and α-tubulin, which inhibits microtubule assembly.[7]

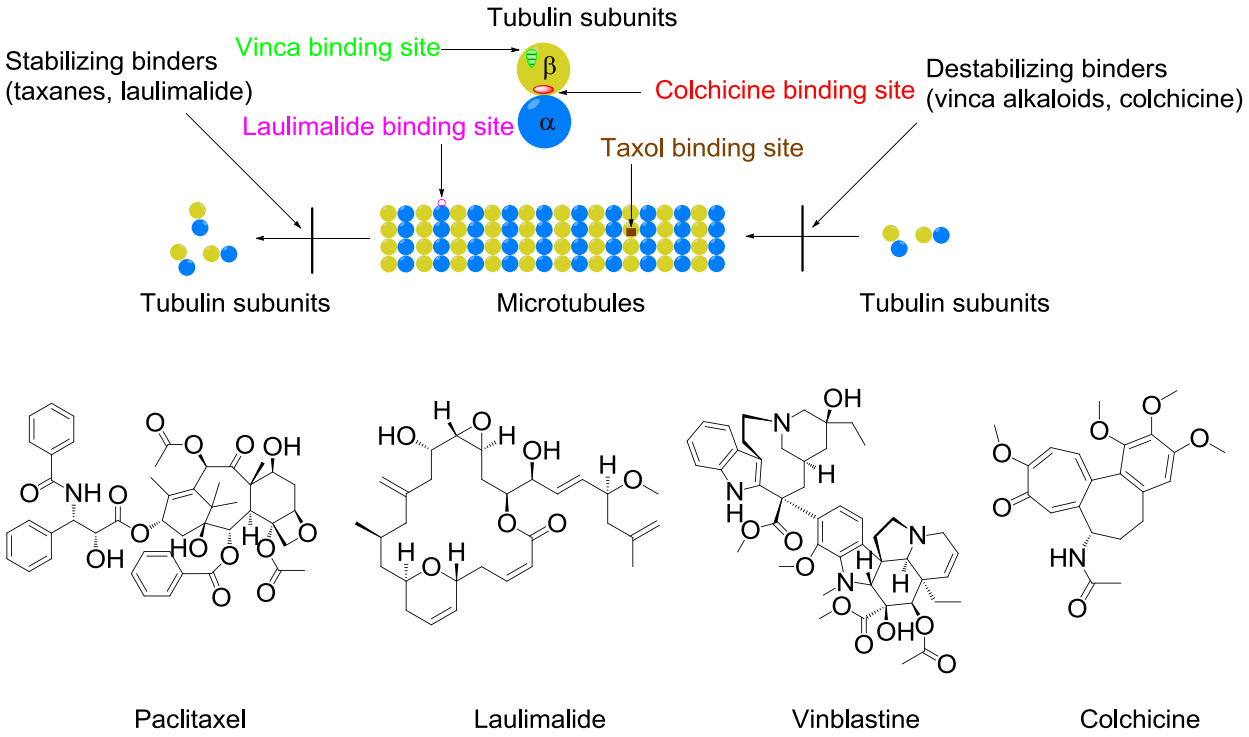

Figure **1.2**: Tubulin binding sites of microtubule targeting agents.

1.2 Tubulin-Binding Agents in Cancer Chemotherapy

Vinca domain-binding agents

Vinca alkaloids were originally isolated from the *Vinca rosea* plant, *Catharanthus roseus*. The first two vinca alkaloids identified, vinblastine and vincristine, are almost structurally identical, except a formyl group is attached to the dihydroindole nitrogen in vincristine, whereas vinblastine has a methyl group at that position. Vinblastine and vincristine bind to the β-subunit of tubulin at a distinct region called the vinca-binding domain,[8] thereby inhibiting the assembly of microtubules. They are usually used to treat breast cancer, testicular cancer, Hodgkin's lymphoma, and small cell lung cancer.[9, 10] Vinorelbine is a semisynthetic derivative of vinblastine, which has an eight-membered ring in the catharanthine moiety instead of the nine-membered ring in the parent vinblastine. This compound has been approved for the treatment of

breast cancer.[11] Vinflunine (Figure 1.3), a novel fluorinated compound obtained by superacid transformation of vinorelbine in the presence of fluorhydric acid, has recently been approved for second-line treatment of bladder cancer.[12]

The dolastatin family, originally isolated from marine peptides of the ocean shell-less mollusc *Dolabella auricularia*, includes dolastatin 10, cemadotin, tasidotin and auristatin PE (Figure 1.3).[13] These agents all associate with the vinca-binding domain of β-tubulin. Phase II clinical trials of dolastatin 10 in patients have been conducted.[14] Performance against solid tumors was lacking, but dolastatin 10 remains a good candidate for developing more active analogues. Auristatin PE (Figure 1.3) is a novel synthetic analogue of dolastatin 10. It maintains potent antitumor activity and is associated with less toxicity than its parent compound dolastatin 10. Moreover, in addition to its efficacy in the inhibition and disruption of the microtubule assembly, auristatin PE has a dual action in blocking blood supply to tumor vasculature.[15] Auristatin PE combines both conventional antitumor activity and distinct antitumor vascular activity to make it a potentially attractive tool for cancer therapy.

Eribulin (Figure 1.3) is a fully synthetic macrocyclic ketone analogue of the marine sponge natural product halichondrin B, which binds in the vinca domain of tubulin.[16] Eribulin exerts its anticancer effects by triggering apoptosis of cancer cells following prolonged and irreversible mitotic blockade.[17] Eribulin mesylate was approved by the U.S. Food and Drug Administration on November 15, 2010, to treat patients with metastatic breast cancer who relapsed after treatment with anthracyclines and taxanes.

Taxane domain-binding agents

Paclitaxel and its semi-synthetic analogue docetaxel were among the most important new additions to the chemotherapeutic arsenal in the late twentieth century. Paclitaxel (taxol, Bristol-Myers Squibb) is a natural product isolated from *Taxus brevifolia*.[18] Docetaxel (taxotere, Sanofi-Aventis) is a water-soluble, semisynthetic analogue of the naturally occurring precursor

10-deacetylbaccatin III, which was isolated from *Taxus baccata*. Both paclitaxel and docetaxel occupy the same binding site in the β-subunit of tubulin called the taxane binding site.[19] Paclitaxel and docetaxel have been used for the treatment of many types of cancer, demonstrating significant activity against solid tumors.[20, 21] Besides paclitaxel and docetaxel, cabazitaxel (Jevtana, Sanofi-Aventis, Figure 1.3) displayed promising results in patients with breast cancer or prostate cancer and has recently been approved by the US Food and Drug Administration for the treatment of metastatic hormone-resistant prostate cancer after the failure of docetaxel treatment.[22]

Epothilones were originally isolated from the myxobacterium *Sorangium cellulosum*. They are a promising novel family of agents for cancer treatment as they are active against taxane-resistant tumors.[23] As of September 2008, epothilones A to F have been identified and characterized. Compared with taxanes, epothilones have good water solubility and do not seem to be substrates for the P-gp efflux pump.[24] Epothilone B (patupilone, Novartis) has been evaluated in clinical trials against a variety of solid tumors. Patupilone crosses the blood-brain barrier and has shown activity in patients with recurrent or progressive brain metastases from non small cell lung cancer (NSCLC).[25]

Ixabepilone (Figure 1.3) is a semi-synthetic derivative of epothilone B. Compared with the parent compound epothilone B, ixabepilone has improved solubility, low plasma protein binding, and high metabolic stability.[26] Like the natural epothilones A and B, ixabepilone stabilizes microtubules and induces apoptosis, and is currently approved for the treatment of advanced taxane-resistant breast cancer in the United States. KOS-862, also known as epothilone D, has a mechanism of action similar to that of taxanes, leading to microtubule stabilization and mitotic arrest. KOS-862 has shown superior in vivo anticancer activity relative to patupilone.[27] In phase 2 trials, KOS-862 showed activity in patients with breast cancer and NSCLC.[28] KOS-1584 (9,10-didehydroepothilone D, Figure 1.3) is a novel analogue of KOS-862. This compound was identified in screens for epothilone analogues with higher potency and

improved pharmacologic and pharmacokinetic (PK) properties. KOS-1584 has shown approximately 3- to 12-fold higher potency compared with KOS-862, enhanced tumor tissue penetration, and reduced exposure to selected tissues including the CNS.[29] An ongoing phase II trial is evaluating the efficacy of KOS-1584 in patients with advanced or metastatic (stage IIIB-IV) NSCLC.[30]

a. Vinca-domain binders

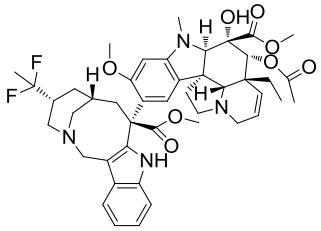

Vinflunine

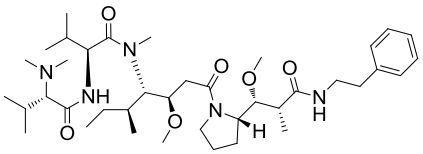

auristatin PE

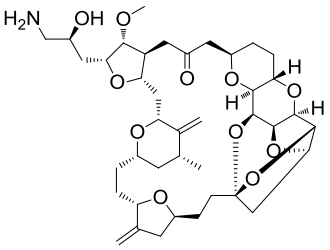

Eribulin

b. Taxane-domain binders

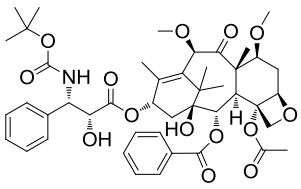

cabazitaxel

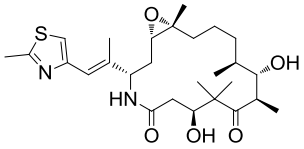

Ixabepilone

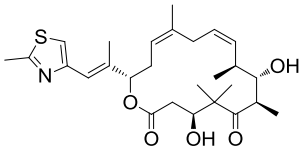

KOS-1584

c. Colchicine-domain binders

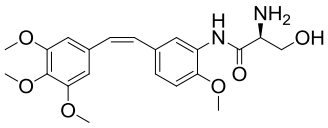

Ombrabulin

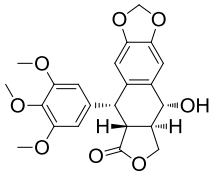

Podophyllotoxin

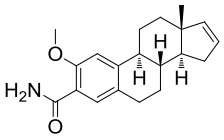

ENMD-1198

d. others

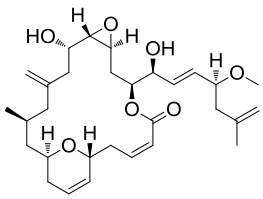

Laulimalide

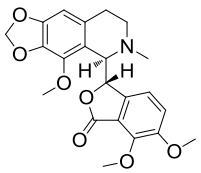

Noscapine

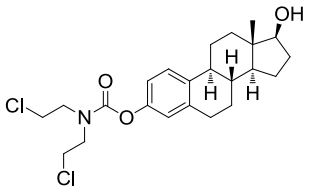

Estramustine

Figure **1.3**: Chemical structures of tubulin-binding agents organized according to their binding domains.

Colchicine domain-binding agents

Colchicine and ZD6126

Colchicine, which was extracted from the poisonous meadow saffron *Colchicum autumnale L*, was the first tubulin destabilizing agent. It has been used for many years as an unapproved drug to treat gout, familial Mediterranean fever and pericarditis.[31] In 2009, U.S. Food and Drug Administration (FDA) approved colchicine as a monotherapy to treat familial Mediterranean fever and acute gout flares. Since cancer cells undergo mitosis at a significantly increased rate, and colchicine can effectively inhibit mitosis, cancer cells are often more susceptible to colchicine poisoning than normal cells. Consequently, colchicine is being investigated as an anticancer drug. However, the therapeutic value of colchicine against cancer is limited by its low therapeutic index.[32]

Since the late 1990s, *N*-acetylcolchicinol-*O*-phosphate (ZD6126), a compound that resembles colchicine and binds in the colchicine site of tubulin, has undergone extensive development as a vascular-disrupting agent.[33] ZD6126 is a water-soluble phosphate prodrug of *N*-acetylcolchinol structurally very similar to colchicine with potential antiangiogenesis and antineoplastic activities.[33] ZD6126 was developed by AstraZeneca for the treatment of metastatic colorectal cancer. However the study was terminated at phase II due to apparent cardiotoxicity at pharmacological doses.[34]

Combretastatin A4 (CA4) and its analogues

Combretastatins are an exciting family of microtubule-targeted agents. They are lead compounds for vascular-targeting agents or vascular-disrupting agents, compounds that produce rapid disruption of tumour blood flow, probably by effects on the microtubule cytoskeleton of endothelial cells. Combretastatin A4 (CA4), isolated from the *Combretum caffrum* tree, is the most potent naturally occurring combretastatin known in regards to both tubulin binding ability and cytotoxicity.[35] However, in Phase I trials, CA4 was found to induce

unusual toxicities such as tumor pain, ataxia and cardiovascular modifications, including prolonged corrected QT interval and electrocardiogram modifications consistent with acute coronary syndrome.[36, 37] CA4P (Zybrestat, fosbretabulin) is the prodrug of CA4 developed by OxiGene. Currently, it is being evaluated in clinical trials as a treatment for solid tumors. Several phase II studies using CA4P have been completed or are ongoing for different type of cancers including anaplastic thyroid cancer, non-small cell lung cancer and relapsed ovarian cancer.[38]

AVE8062 (ombrabulin, Figure 1.3) is another CA4 analogue which exerts its anticancer activity through disrupting blood vessel formation in tumors. Compared with CA4, it has improved water solubility and is orally available. It is effective against a number of cancer cells that are resistant to taxanes.[39] In a phase I study, the combination of AVE8062 with docetaxel was well tolerated. A phase III study is currently ongoing for advanced cancer treatment.[40]

Phenstatin is another CA4 analogue with the double bond of CA4 replaced by a carbonyl group. Phenstatin showed strong cytotoxicity and antitubulin activity similar to CA4, but it is more stable compared with CA4, which is unstable *in vivo* due to the transformation from the active cis-configuration to the more stable but inactive trans-configuration.[41] CC-5079 is a 1,1-diarylethene analogue of CA4, which is called isocombretastatin A. CC-5079 has dual inhibitory activity against tubulin polymerization and phosphodiesterase-4 (PDE4). It shows both antiangiogenic and antitumor activities. CC-5079 can arrest cell cycle in the G2/M phase, increase phosphorylation of G2/M checkpoint proteins, and induce apoptosis.[42]

Miscellaneous agents targeting the colchicine binding site

Podophyllotoxin (Figure 1.3), otherwise known as podofilox, is a non-alkaloid toxic lignan extracted from the roots and rhizomes of *Podophyllum* species. Podophyllotoxin competitively inhibits binding of colchicine to tubulin. It binds to tubulin more rapidly than colchicine does. The utilization of Podophyllotoxin as a lead in drug design has resulted in useful cancer fighting drugs such asetoposide, teniposide, and etoposidephosphate.[43]

Steganacin, a new lignan lactone from the alcoholic extract of Steganataenia araliacea Hochest, has significant antitumor activity in vivo against P388 leukemia cells in mice and in vitro against cells derived from a human carcinoma of the nasopharynx (KB).[44] Steganacin prevents the formation of the spindle. This suggested that steganacin, like other spindle poisons such as colchicine and podophyllotoxin, exerts its antimitotic activity through an effect on spindle microtubules.[44]

Curacin A, originally purified as a major lipid component from a strain of the cyano bacterium *Lyngbya majuscule* isolated in Curaçao, is a potent inhibitor of cell growth and mitosis. It binds rapidly and tightly at the colchicine site of tubulin.[45] Poor water-solubility and lack of chemical stability prevent the clinical development of curacin A, but synthetic analogues with improved bioavailability may provide more promise.

2-Methoxyestradiol (2-ME) is an endogenous estrogen metabolite, formed by hepatic cytochrome P450 2-hydroxylation of β-estradiol and 2-O-methylation via catechol O-methyltransferase. This metabolite has attracted interest because of its potent inhibition of tumor vasculature and tumor cell growth.[46] Studies have shown that 2-ME is metabolized by conjugation at positions 3 and 17 and oxidation at position 17, forming inactive metabolites. In order to make metabolically stable analogues with improved anti-tubulin properties, ENMD-1198 (Figure 1.3) was generated via chemical modification at 3 and 17 position. This agent also binds to the colchicine binding site in tubulin. Studies showed that ENMD-1198 was very potent at inhibiting endothelial cell proliferation, motility, migration, and morphogenesis. Furthermore, ENMD-1198 is able to quickly disrupt vascular structures.[47]

Other tubulin-binding agents

Laulimalide (Figure 1.3) is a potent, structurally unique microtubule-stabilizing agent originally isolated from the marine sponge *Cacospongia mycofijiensis*.[48] Laulimalide exhibits an activity profile different from other microtubule-binding agents, notably including effectiveness

against paclitaxel-resistant cells. Unfortunately, laulimalide has a narrow therapeutic index and is intrinsically unstable; therefore it is considered unsuitable for clinical trials.

Noscapine (Figure 1.3) is an alkaloid from plants of the Papaveraceae family. Currently, phase I/II clinical trials with noscapine for non–Hodgkin's lymphoma and multiple myeloma are in progress (ClinicalTrials.gov identifier: NCT00912899). Furthermore, several analogues of noscapine with increased potency in humans are under investigation as cancer therapeutics.[49]

Estramustine (Figure 1.3) is a chemotherapy agent used for the treatment of prostate carcinoma. Estramustine inhibits growth and induces mitotic arrest in many types of cultured cells, including the human prostate carcinoma cell lines DU 145 and PC3. It was reported that the antimitotic mechanism of action of estramustine may be due to binding to a novel site in tubulin and stabilization of microtubule dynamics.[50]

Table **1.1**: Tubulin-binding agents, their diverse binding sites and therapeutic uses.

Binding domain	Related drugs or analogues	Therapeutic uses	References
Vinca domain	Vinblastine	Hodgkin's lymphoma, testicular cancer	9
	Vincristine	Leukaemia, small cell lung cancer	10
	Vinorelbine	Breast cancer	11
	Vinflunine	Bladder cancer	12
	Dolastatins (such as auristatin PE)	Potential vascular-targeting agent	13-15
	Eribulin mesylate	Metastatic breast cancer	16-17
Taxane domain	Paclitaxel	Lung, breast and ovarian	20

		cancer	
	Docetaxel	Breast and prostate cancer	21
	Cabazitaxel	Breast and prostate cancer	22
	Epothilone B	Non small cell lung cancer	25
	Ixabepilone	Taxane-resistant breast cancer	26
	Epothilone D	Breast and lung cancer	27, 28
	KOS-1584	Non small cell lung cancer	29, 30
Colchicine domain	Colchicine	Non-neoplastic diseases (gout, familial Mediterranean fever)	31
	ZD6126	Colorectal cancer	33
	Combretastatins (CA4, CA4P, Ombrabulin, Phenstatin, CC-5079)	Vascular-targetting agents for the treatment of many types of cancer	35-42
	Steganacin	Nasopharynx cancer	44
	2-Methoxyestradiol and its analogue ENMD-1198	Ovarian cancer	46, 47
Other binding sites	Laulimalide	N/A	48
	Noscapine	Non–Hodgkin's lymphoma	49
	Estramustine	Prostate cancer	50

1.3 Limitations of Tubulin-Binding Agents in Cancer Chemotherapy

Three major shortcomings limit the application of tubulin-binding agents in cancer chemotherapy. These include undesired toxicity, poor tissue specificity and drug resistance. Among the side effects caused by tubulin-binding agents, neuropathy is a chief limitation in the use of these agents.[51] For example, vincristine induces neurotoxicity characterized by a peripheral, symmetric mixed sensory-motor, and autonomic polyneuropathy.[52] Hematopoietic toxicity is also frequently observed with microtubule-targeted agents, with subtle differences between compounds in the same family. For example, in phase I studies neutropenia was one of the dose-limiting toxicities observed with ixabepilone.[53]

Another major limitation of using tubulin-targeting agents clinically is innate and acquired drug resistance. The most common form of clinical resistance is over-expression of the MDR1 gene, which encodes the P-glycoprotein (Pgp) drug efflux pump.[54] This membrane-associated ATP-binding cassette (ABC) transporter is over expressed in many tumor cell lines, including tissues of the liver, kidney, and gastrointestinal tract. Over-expression of Pgp decreases intracellular drug levels and is associated with poor response to tubulin-binding agents including taxanes and vinca alkaloids.[55] Besides over-expression of ABC transporters, over-expression of the βIII-tubulin isoform is another significant mechanism of resistance. Among the eight identified β-tubulin isotypes in humans, over-expression of class III β-tubulin promotes resistance to tubulin-binding agents such as paclitaxel and vinorelbine.[56] Clinical development of new tubulin-binding agents that circumvents both of these drug resistance mechanisms could have advantages for patients with drug resistant tumors.

1.4 Future Development of Tubulin-Binding Agents

Microtubules are a highly-validated target in cancer therapy. Consequently, many efforts have been made to develop novel agents directed against this target. The development of novel tubulin-binding agents with better properties is of significant interest.

One approach is focused on the discovery tubulin-binding agents that are not substrates for efflux pumps and other modifications of drugs to confer lower affinity for transporting proteins. Several promising agents have been reported in preclinical studies. These include peloruside A, taccalonolides, coumarins and cyclostreptin (Figure 1.4).[57]

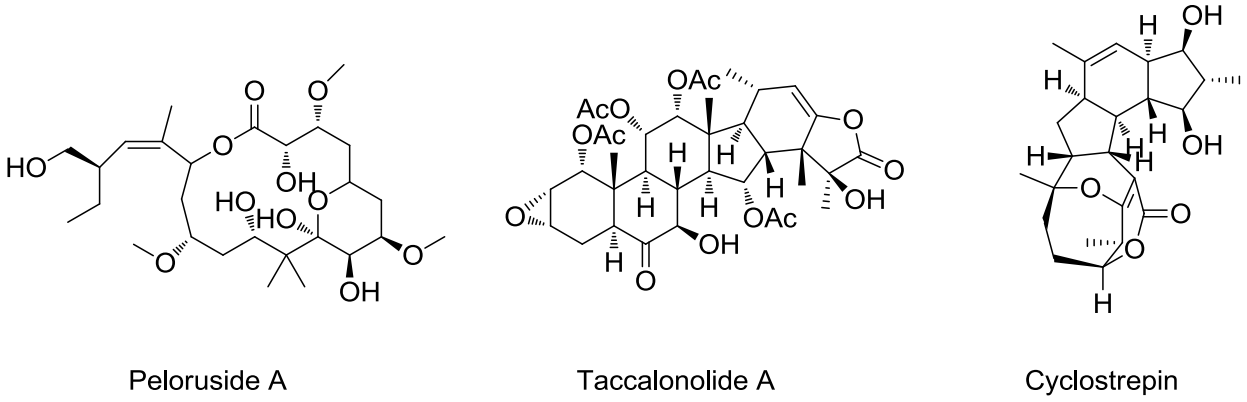

Figure **1.4:** Chemical structures of peloruside A, taccalonolide A and cyclostrepin.

The tumor vasculature is an attractive new target for cancer therapy. An advantage is the relatively easy access of therapeutic agents to the target. It is known that some compounds can inhibit the formation of new blood vessels (inhibit the process of angiogenesis) or shut down existing ones. Tumor cells die quickly after cutting off the oxygen supply. Moreover, some of these agents act only with tumor vasculature and do not interact with normal tissues. Many anti-vascular agents are similar to colchicine and bind to the colchicine binding site on β-tubulin. Development of novel agents targeting the colchicine binding site (which is not used by any currently approved anticancer drugs) may be a promising approach.[58]

Another attractive strategy involves vectorization of tubulin-binding agents to tumor cells using delivery systems, such as liposomes, polymers, antibodies, or cell-penetrating peptides.[59] Maytansine is a potent tubulin-binding agent that induces mitotic arrest and kills tumor cells at subnanomolar concentrations. However, its side effects and lack of tumor specificity have prevented successful clinical use. Antibody-conjugated maytansine derivatives have been developed to overcome these drawbacks. Trastuzumab–DM1, a maytansinoid conjugated to trastuzumab, a therapeutic antibody targeting the human epidermal growth factor receptor 2 (ERBB2) has show good efficacy in clinical trials against metastatic breast cancer.[59]

1.5 Conclusion

Tubulin-binding agents are an important class of compounds for cancer chemotherapy. Disparities in their tubulin binding properties lead to differences in their mechanisms of action with a significant impact on the efficacy or toxicity profile of each agent. Because of numerous adverse effects and limitations in use, new tubulin-binding agents with better properties are needed. Especially desired are improvements in antitumor activity, toxicity profile, drug formulation, and pharmacology. Among the approaches for development of novel tubulin-binding agents with better properties, modifying these agents with delivery systems has significant promise. Delivery systems might enable considerable amounts of tubulin-binding agents to be administrated to the tumor without toxic effects towards normal tissues. Research on binary systems designed to deliver tubulin-binding agents into early endosomes of tumor cells and release these agents is described in this thesis.

1.6 Reference

1. Nogales E. Structural insight into microtubule function. *Annu*. *Rev*. *Biophys*. *Biomol*. *Struct*. **2001**, *30*, 397-420.

2. Zhou, J.; Giannakakou, P. Targeting microtubules for cancer chemotherapy. *Curr*. *Med*. *Chem. Anticancer Agents* **2005**, *5*, 65-71.

3. Attard, G.; Greystoke, A.; Kaye, S.; De Bono, J. Update on tubulin-binding agents. *Pathol. Biol.* **2006**, *54*, 72-84.

4. Pryor, D. E.; O'Brate, A.; Bilcer, G.; Diaz, J. F.; Wang, Y.; Kabaki, M. The microtubule stabilizing agent laulimalide does not bind in the taxoid site, kills cells resistant to paclitaxel and epothilones, and may not require its epoxide moiety for activity. *Biochemistry* **2002**, *41*, 9109-9115.

5. Schiff, P. B., Fant, J. & Horwitz, S. B. Promotion of microtubule assembly in vitro by taxol. *Nature* **1979**, *277*, 665–667.

6. Gigant, B.; Wang, C.; Ravelli, R. B.; Roussi, F.; Steinmetz, M. O.; Curmi, P. A. Structural basis for the regulation of tubulin by vinblastine. *Nature* **2005**, *435*, 519-522.

7. Ravelli, R. B.; Gigant, B.; Curmi, P. A.; Jourdain, I.; Lachkar, S.; Sobel, A. Insight into tubulin regulation from a complex with colchicines and a stathmin-like domain. *Nature* **2004**, *428*, 198-202.

8. Bai, R. B.; Pettit, G. R.; Hamel, E. Binding of dolastatin 10 to tubulin at a distinct site for peptide antimitotic agents near the exchangeable nucleotide and Vinca alkaloid sites. *J. Biol. Chem*. **1990**, *265*, 17141-17149.

9. Little, R.; Wittes, R. E.; Longo, D. L.; Wilson, W. H. Vinblastine for recurrent Hodgkin's disease following autologous bone marrow transplant. *J*. *Clin*. *Oncol.* **1998**, *16*, 584-588.

10. Sandler, A. B. Chemotherapy for small cell lung cancer. *Semin. Oncol*. **2003**, *30*, 9-25.

11. Rossi, A. et al. Single agent vinorelbine as first-line chemotherapy in elderly patients with advanced breast cancer. *Anticancer Res*. **2003**, *23*, 1657-1664.

12. Bellmunt, J. et al. Phase III trial of vinflunine plus best supportive care compared with best supportive care alone after a platinum-containing regimen in patients with advanced transitional cell carcinoma of the urothelial tract. *J. Clin. Oncol*. **2009**, *27*, 4454-4461.

13. Cormier, A.; Marchand, M.; Ravelli, R. B.; Knossow, M.; Gigant, B. Structural insight into the inhibition of tubulin by vinca domain peptide ligands. *The EMBO journal* **2008**, *9*, 1101-1106.

14. Rogatko, A. et al. Phase II Trial of Dolastatin-10, a Novel Anti-Tubulin Agent, in Metastatic Soft Tissue Sarcomas. *Sarcoma* **2004**, *8*, 107-111.

15. Natsume, T.; Watanabe, J.; Tamaoki, S.; Fujio, N.; Miyasaka, K.; Kobayashi, M. J. Characterization of the Interaction of TZT-1027, a Potent Antitumor Agent, with Tubulin. *Cancer Res*. **2000**, *91*, 737–747.

16. Bai, R. L.; Paull, K. D.; Herald, C. L.; Malspeis, L.; Pettit, G. R,; Hamel E. Halichondrin B and homohalichondrin B, marine natural products binding in the vinca domain of tubulin. Discovery of tubulin-based mechanism of action by analysis of differential cytotoxicity data. *J. Biol. Chem.* **1991**, *266*, 15882-15889.

17. Towle, M. J.; Salvato, K. A.; Wels, B. F.; Aalfs, K. K.; Zheng, W.; Seletsky, B. M.; Zhu, X.; Lewis, B. M.; Kishi, Y.; Yu, M. J.; Littlefield, B. A. Eribulin induces irreversible mitotic blockade: implications of cell-based pharmacodynamics for in vivo efficacy under intermittent dosing conditions. *Cancer Res*. **2011**, *71*, 496-505.

18. Wani, M. C.; Taylor, H. L.; Wall, M. E. Plant antitumor agents. VI. The isolation and structure of taxol, a novel antileukemic and antitumor agent from Taxus brevifolia. *J. Am. Chem. Soc*. **1971**, *93*, 2325-2327.

19. Nogales, E.; Wolf, S. G.; Khan, I. A.; Ludueña, R. F.; Downing, K. H. Structure of tubulin at 6.5 Å and location of the taxol-binding site. *Nature* **1995**, *375*, 424-427.

20. Sanjeev, K.; Adnan, M. Clinical trials and progress with paclitaxel in ovarian cancer. *Int. J. Womens Health* **2010**, *2*, 411–427.

21. Lyseng-Williamson, K. A.; Fenton, C. Docetaxel: a review of its use in metastatic breast cancer. Drugs **2005**, *65*, 2513-2531.

22. Sampath, D. et al. MAC-321, a novel taxane with greater efficacy than paclitaxel and docetaxel in vitro and in vivo. *Mol. Cancer Ther*. **2003**, *2*, 873-884.

23. Chou, T. C. et al. Desoxyepothilone B is curative against human tumor xenografts that are refractory to paclitaxel. *Proc. Natl Acad. Sci*. **1998**, *95*, 15798-15802.

24. Lee, J. J.; Swain, S. M. Development of novel chemotherapeutic agents to evade the mechanisms of multidrug resistance (MDR). *Semin. Oncol*. **2005**, *32*, S22–S26.

25. Abrey, L.; Wen, P. Y.; Govindan, R. Activity of patupilone for the treatment of recurrent or progressive brain metastases in patients (pts) with non-small cell lung cancer (NSCLC): an open-label, multicenter, phase II study. *J. Clin. Oncol*. **2007**, *25*, 18058.

26. Lee, F. Y.; Smykla, R.; Johnston, K. Preclinical efficacy spectrum and pharmacokinetics of ixabepilone. *Cancer Chemother. Pharmacol*. **2009**, *63*, 201-212.

27. Fumoleau, P.; Coudert, B.; Isambert, N.; Ferrant, E. Novel tubulin-targeting agents: anticancer activity and pharmacologic profile of epothilones and related analogues. *Ann. Oncol*. **2007**, *18*, v9-15.

28. Overmoyer, B.; Waintraub, S.; Kaufman, P. A. Phase II trial of KOS-862 (epothilone D) in anthracycline and taxane pretreated metastatic breast cancer. *J. Clin. Oncol*. **2005**, *23*, 778.

29. Zhou, Y.; Zhong, Z.; Liu, F. KOS-1584: a rationally designed epothilone D analogue with improved potency and pharmacokinetic (PK) properties. *Proc. Am. Assoc. Cancer Res*. **2005**, *46*, 2535.

30. Study to evaluate KOS-1584 in patients with advanced or metastatic (stage IIIB/IV) non-small cell lung cancer [accessed 2009 Jan 19]. Available from: http://clinicaltrials.gov/ct2/show/NCT00651508.

31. Wallace, G.; James, B. R. Intravenous colchicine in the treatment of gouty arthritis. *Ann. Rheum. Dis*. **1953**, *12*, 16-19.

32. Horton, R. A.; Bagnato, J. D.; Grissom, C, B. Synthesis and characterization of a cobalamin-colchicine conjugate as a novel tumor-targeted cytotoxin. *J. Org. Chem*. **2004**, *69*, 8987-8996.

33**.** Goto, H.; Yano, S.; Zhang, H.; Matsumori, Y.; Ogawa, H.; Blakey, D. C. Activity of a new vascular targeting agent, ZD6126, in pulmonary metastases by human lung adenocarcinoma in nude mice. *Cancer Res*. **2002**, *62*, 3711-3715.

34. AstraZeneneca. http://www.astrazeneca.com/sites/7/imagebank/typeArticleparam511672/astrazeneca-2005-annual-report.pdf [accessed August 2006].

35. Griggs, J.; Metcalfe, J. C.; Hesketh, R. Targeting tumour vasculature: the development of combretastatin A4. *Lancet Oncol*. **2001**, *2*, 82-87.

36. Rustin, G. J. et al. Phase I clinical trial of weekly combretastatin A4 phosphate: clinical and pharmacokinetic results. *J. Clin. Oncol*. **2003**, *21*, 2815-2822.

37. Cooney, M. M. et al. Cardiovascular safety profile of combretastatin a4 phosphate in a single-dose Phase I study in patients with advanced cancer. *Clin. Cancer Res*. **2004**, *10*, 96-100.

38. Rustin, G. J.; Shreeves, G.; Nathan, P. D.; Gaya, A.; Ganesan, T. S.; Wang, D. A Phase Ib trial of CA4P (combretastatin A-4 phosphate), carboplatin, and paclitaxel in patients with advanced cancer. *Br. J. Cancer* **2010**, *102*, 1355-1360.

39. Kim, T. J.; Ravoori, M.; Landen, C. N.; Kamat, A. A.; Han, L. Y.; Lu, C. Antitumor and antivascular effects of AVE8062 in ovarian carcinoma. *Cancer Res*. **2007**, *67*, 9337-9345.

40. https://www.sanofioncology.com/pipeline/ombrabulin.aspx

41. Pettit, G. R.; Toki, B.; Herald, D. L.; Verdier-Pinard, P.; Boyd, M. R.; Hamel, E. Antineoplastic agents. 379. Synthesis of phenstatin phosphate. *J. Med. Chem*. **1998**, *41*, 1688-1695.

42. Zhang, L. H.; Wu, L.; Raymon, H. K.; Chen, R. S.; Corral, L.; Shirley, M. A. The synthetic compound CC-5079 is a potent inhibitor of tubulin polymerization and tumor necrosis factor-alpha production with antitumor activity. *Cancer Res*. **2006**, *66*, 951-959.

43. Bohlinand L, Rosen B. Podophyllotoxin derivatives: drug discovery and development. *Drug Discov. Today* **1996**, *1*, 343-351.

44. Kupchan, S. M.; Britton, R. W.; Ziegler, M. F.; Gilmore, C. J.; Restivo, R. J.; Bryan, R. F. Steganacin and steganangin, novel antileukemic lignan lactones from Steganotaenia araliacea. *J. Am. Chem. Soc.* **1973**, *95*, 1335-1336.

45. Hamel E. Antimitotic natural products and their interactions with tubulin. *Medicinal Research Reviews* **1996**, *16*, 207-231.

46. Matei, D.; Schilder, J.; Sutton, G.; Perkins, S.; Breen, T.; Quon, C. Activity of 2-methoxyestradiol (Panzem NCD) in advanced, platinumresistant ovarian cancer and primary peritoneal carcinomatosis: a Hoosier Oncology Group trial. *Gynecol Oncol*. **2009**, *115*, 90-96.

47. Pasquier, E.; Sinnappan, S.; Munoz, M. A.; Kavallaris, M. ENMD-1198, a new analogue of 2-methoxyestradiol, displays both antiangiogenic and vascular-disrupting properties. *Mol. Cancer Ther*. **2010**, *9*, 1408-1418.

48. Mooberry, S. L.; Tien, G.; Hernandez, A. H.; Plubrukarn, A.; Davidson, B. S. Laulimalide and Isolaulimalide, New Paclitaxel-Like Microtubule-Stabilizing Agents. *Cancer Res.* **1999**, *59***,** 653-660.

49. Mishra, R. C.; Karna, P.; Gundala, S. R.; Pannu, V.; Aneja, R. Second generation benzofuranone ring substituted noscapine analogues: synthesis and biological evaluation. *Biochem Pharmacol.* **2011**, *82*, 110-121.

50. Panda, D.; Miller, H. P.; Islam, K.; Wilson, L. Stabilization of microtubule dynamics by estramustine by binding to a novel site in tubulin: A possible mechanistic basis for its antitumor action. *Proc. Natl. Acad. Sci. USA*. **1997**, *94*, 10560-10564.

51. Canta, A.; Chiorazzi, A.; Cavaletti, G. Tubulin: a target for antineoplastic drugs into the cancer cells but also in the peripheral nervous system. *Curr. Med. Chem*. **2009**, *16*, 1315-1324.

52. Quasthoff, S.; Hartung, H. P. Chemotherapy-induced peripheral neuropathy. *J. Neurol*. **2002**, *249*, 9-17.

53. Aghajanian, C. et al. Phase I study of the novel epothilone analogue ixabepilone (BMS-247550) in patients with advanced solid tumors and lymphomas. *J. Clin. Oncol*. **2007**, *25*, 1082–1088.

54. Aller, S. G.; Yu, J.; Ward, A.; Weng, Y.; Chittaboina, S; Zhuo, R.; Harrell, P. M.; Trinh, Y. T.; Zhang, Q.; Urbatsch, I.L.; Chang, G. Structure of P-glycoprotein reveals a molecular basis for poly-specific drug binding. *Science* **2009**, *323*, 1718-1722.

55. Drukman, S.; Kavallaris, M. Microtubule alterations and resistance to tubulin-binding agents. *Int. J. Oncol.* **2002**, *21*, 621-628.

56. Stengel, C.; Newman, S. P.; Leese, M. P.; Potter, B. V.; Reed, M. J. Purohit, A. Class III beta-tubulin expression and in vitro resistance to microtubule targeting agents. *Br. J. Cancer* **2010**, *102*, 316-324.

57. Charles, D.; Mary, A. G. Microtubule-binding agents: a dynamic field of cancer therapeutics. *Nat. Rev. Drug Discov*. **2010**, *9*, 791-803.

58. Jordan, M. A.Mechanism of Action of Antitumor Drugs that Interact with Microtubules and Tubulin. *Curr. Med. Chem. AntiCancer Agents* **2002**, *2*, 1-17

59. Krop, I. E. Phase I study of trastuzumab-DM1, an HER2 antibody-drug conjugate, given every 3 weeks to patients with HER2-positive metastatic breast cancer. *J. Clin. Oncol*. **2010**, *28*, 2698–2704.

Chapter 2. A Binary Drug Delivery System: Release of Disulfide-Linked Tubulin-Binding Agents Mediated by Endosome Disruptive Peptides

2.1 Introduction

Drug delivery is an important field in the pharmaceutical sciences. Controlled drug delivery can improve bioavailability by preventing metabolism and enhancing cellular uptake. By controlling the rate of drug release, drug delivery systems can maintain drug concentrations within a therapeutic window and reduce side effects by targeting of drugs to diseased tissues and cells.[1]

Historically, therapeutic agents have predominately comprised small molecules with molecular weights below a few hundred. However, recent advances have led to the discovery of novel therapeutics including proteins, monoclonal antibodies, and nucleic acids.[2-4] Most of these agents are impermeable to cell membranes and delivery into cells poses new challenges beyond those encountered with traditional small-molecule therapeutics. To circumvent membrane barriers, some of these agents have been combined with delivery systems such as liposomes,[5] polymers,[6] cell-penetrating peptides (CPPs),[7, 8] or include ligands targeting internalizing cell surface receptors.[9-11] However, the underlying mechanisms of these methods are often not well understood, and the delivery efficiencies of these methods vary substantially.

Receptor-mediated endocytosis (RME) is a major mechanism used by mammalian cells for the uptake of macromolecules from extracellular fluid.[12] RME of cholesterol-laden LDL particles by the LDL receptor (LDLR) has been extensively characterized,[13,14] and key features of this process are illustrated in Figure 2.1. In this process, extracellular ligands (LDL particles) bind the LDL receptor, a natural cell surface receptor that clusters in dynamic regions of cellular plasma membranes. By actively pinching off to form intracellular vesicles, these membrane

micro domains are internalized, encapsulating ligand-receptor complexes in the cytoplasm. These vesicles fuse to form early/sorting endosomes that are acidified (pH ~ 6) through the activation of proton pumps, conditions that promote the dissociation of many ligands from receptors. Free receptors often traffic back to the cell surface through related recycling endosomes.[15] Meanwhile, dissociated ligands are generally transported to more acidic late endosomes and lysosomes (pH ~ 5), where hydrolases and other enzymes promote their degradation.

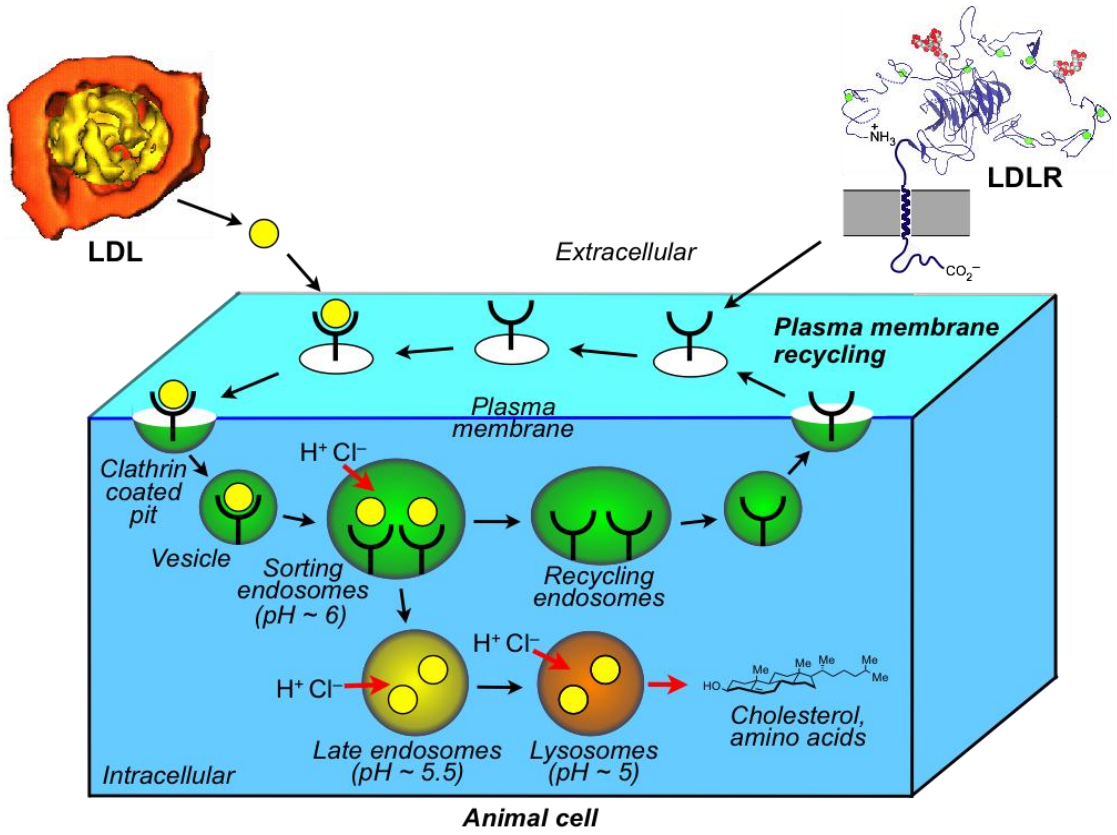

Figure **2.1**: Receptor-mediated endocytosis of the LDL in animal cell. Figure courtesy of Professor Blake R. Peterson.

Because of the high abundance of cholesterol in cellular plasma membranes, and its role in cycling between the cell surface and early/recycling endosomes,[16] our group has focused

on using analogues of cholesterol, particularly derivatives of cholesterylamine, to construct synthetic compounds that mimic cellular uptake and trafficking properties of natural cell surface receptors.[17] Cholesterol derivatives have been used to facilitate the delivery of siRNA,[18] enhance DNA transfection,[19] probe cellular membrane subdomains,[20] and have been proposed for tumor targeting applications.[21] The cationic cholesterol mimic 3β-amino-5-cholestene (3β-cholesterylamine, **1**, Figure 2.2) is of particular interest because of its high affinity for phospholipid membranes.[22] Derivatives of 3β-amino-5-cholestene have been used to construct photoaffinity probes[23] and related aminosteroids.[24] *N*-Alkyl derivatives of 3β-amino-5-cholestene can insert into plasma membranes of living mammalian cells and cycle between the cell surface and early/recycling endosomes, mimicking the membrane trafficking of many cell surface receptors.[25]

Cargo linked to *N*-alkyl-3β-cholesterylamines and many other delivery systems can become trapped in endosomes of living mammalian cells. Because many biologically active molecules have targets either in the cytoplasm or nucleus, the entrapment of these molecules in endosomes can limit efficacy. To address this problem, several approaches for disruption of endosomes have been explored. Many viruses enter host cells via endocytic mechanisms and use specific molecules on viral capsid, called fusion proteins (FPs), to disrupt endosomes and release genetic material into the cytoplasm.[26] To mimic this endosome disruption strategy, viral fusion proteins have been incorporated into liposomes, [27] combined with polymers, [28] or linked to CPPs[29] to facilitate the release of cargo molecules. Although these peptides can be prepared on solid phase, the subtantial length of many these peptides makes the synthesis costly, and some of these peptides are toxic to cells. In 2006, Thomas Weber and his coworkers identified a pH-dependent lytic peptide termed PC4 (**2**, Figure 2.2), using phage display technology.[30] PC4 was shown to promote pH-dependent leakage of compounds from liposomes comparable to some viral fusion peptides, but this peptide is significantly smaller than most viral peptides (12 amino acids). Inspired by studies of PC4, our group designed and synthesized an *N*-alkyl-3β-

cholesterylamine-capped membrane lytic peptide (cholesterylamine-PC4, **3**, Figure 2.2). To investigate whether this compound (**3**) can promote endosome disruption and release of cargo trapped in early/recycling endosomes, we designed and synthesized another derivative of *N*-alkyl-3β-cholesterylamine comprising the green fluorophore 5-carboxyfluorescein linked through a disulfide bond (**4**, Figure 2.2).

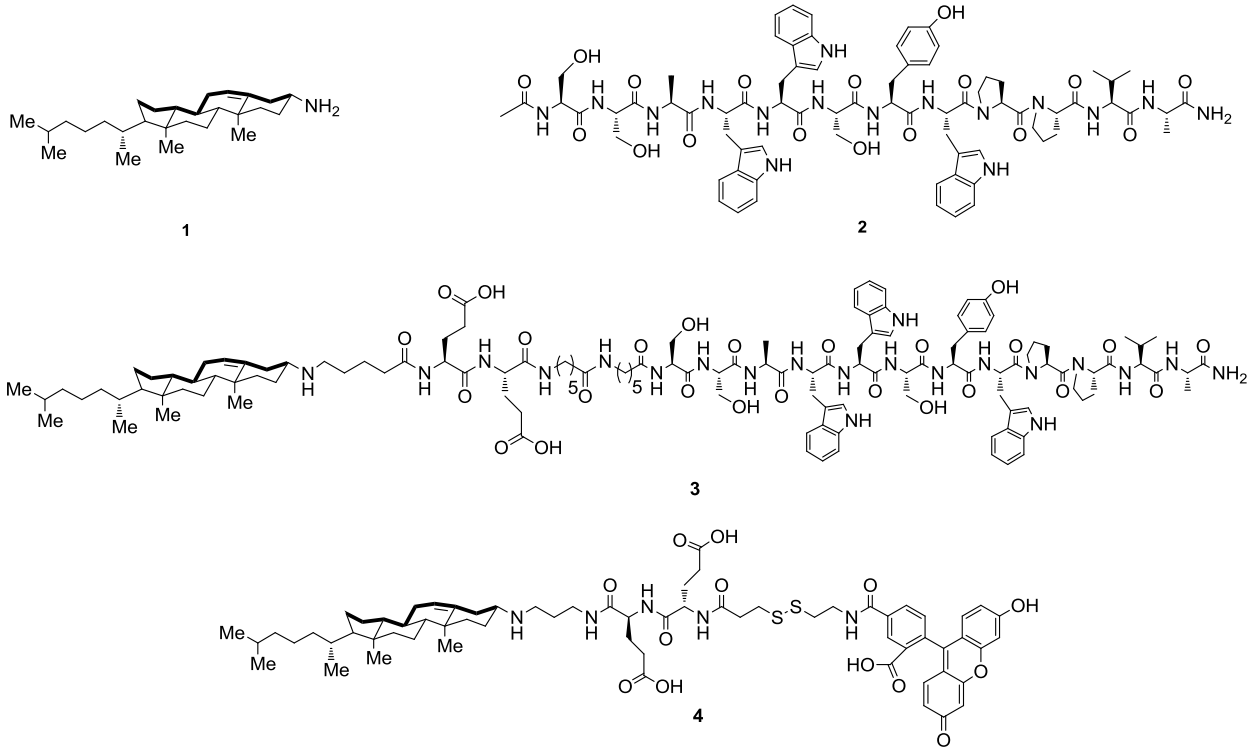

Figure **2.2**: Structures of 3β-cholesterylamine (**1**), PC4 (**2**), cholesterylamine-PC4 (**3**) and disulfide probe (**4**).

We hypothesized that when added to mammalian cells, derivatives of *N*-alkyl-3β-cholesterylamine would become incorporated in cellular plasma membranes and engage a membrane trafficking pathway that involves rapid cycling between the cell surface and intracellular endosomes, similar to many natural cell surface receptors.[25] Because early/recycling endosomes are thought to be oxidizing,[31] we hypothesized that the disulfide bond of **4** should be relatively stable in these compartments. However, if compound **4** were exposed to reduced glutathione (GSH), a thiol present at mM concentrations in the cytosol, this

functional group would be cleaved.[32] Correspondingly, disruption of early/recycling endosomes loaded with **4** by compound **3** was proposed as a mechanism to enable GSH to access these compartments, reduce the disulfide bond of **4,** and release the soluble fluorophore **5** into the cytoplasm and nucleus of cells (Figure 2.3). [33]

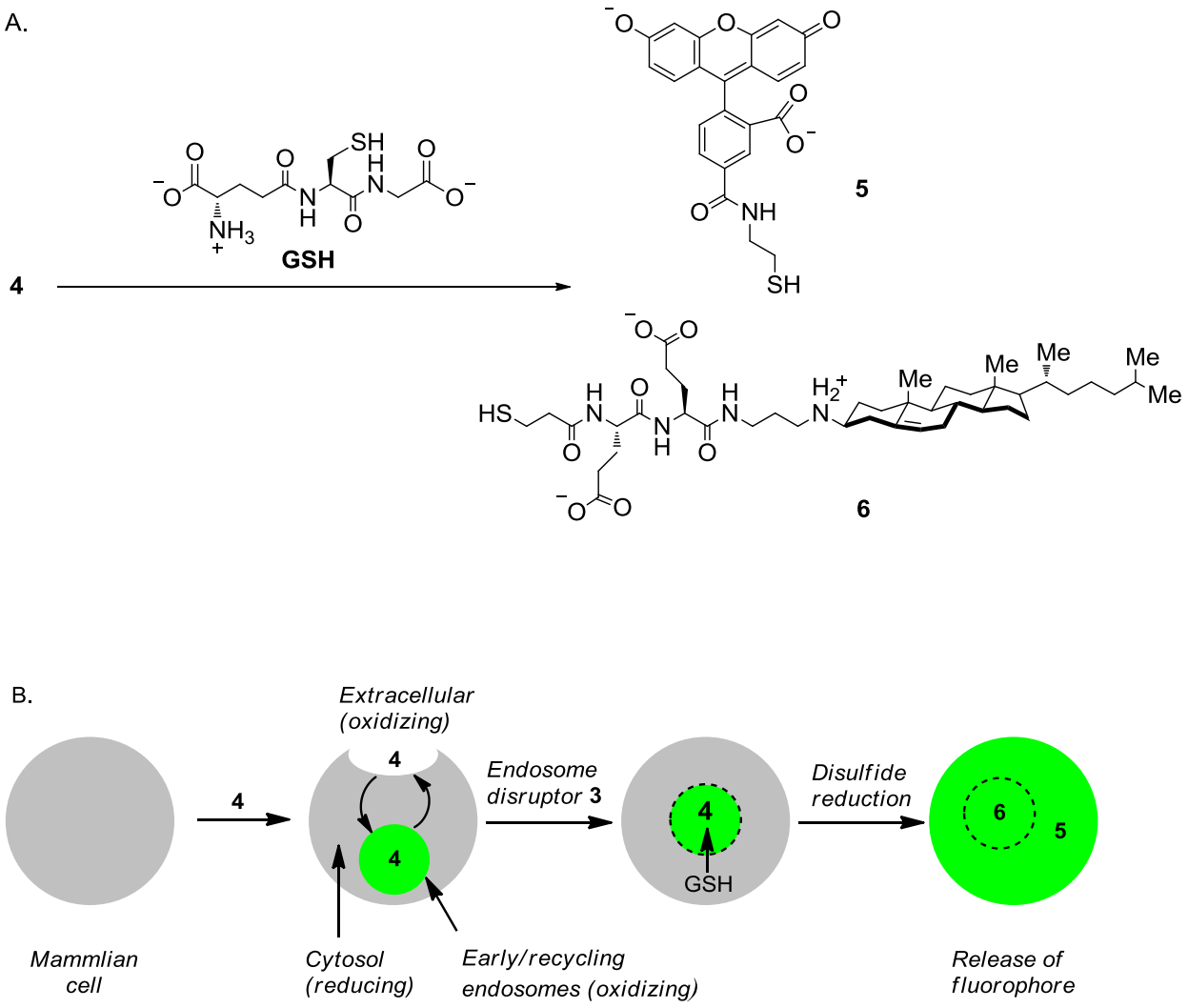

Figure **2.3**: Proposed molecular mechanism for the selective release of disulfide-linker fluorophore from early/recycling endosomes mediated by **3.** Panel A: Products of cleavage of **4** by glutathione. Panel B: Mechanism of release of fluorophore **5** into the cytosol and nucleus of mammalian cells.

To investigate this concept, living Jurkat lymphocytes were treated with molecular probe **4** in the presence or absence of the cholesterylamine-PC4 lipopeptide (**3**). Confocal laser scanning microscopy revealed that, when combined with **3,** the green fluorescence of **4** was released from entrapment in early/recycling endosomes and fluorescence was observed the cytosol and nucleus (Figure 2.4).[33]

A. Treatment for 12 h with: **4** (2.5 µM) B. Treatment for 12 h with: **4** (2.5 µM) + **3** (2 µM)

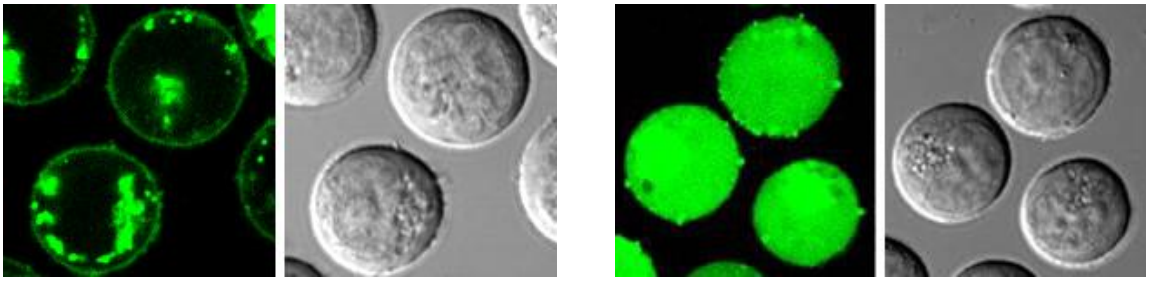

Figure **2.4**: Confocal laser scanning and DIC micrographs of living Jurkat lymphocytes treated with cholesterylamine-PC4 (**3**) and disulfide probe (**4**). Panel A: Jurkat lymphocytes were treated with **4** only (2.5 µM) for 12 h at 37 ^{o}C. Panel B: Jurkat lymphocytes were treated with **3** (2 µM) and **4** (2.5 µM) for 12 h at 37 ^{o}C. Adapted from Sun, Q., Cai, S., Peterson, B. *J. Am. Chem. Soc*. **2008**, *130*, 10064-10065.

Starting with cholesterylamine-PC4 (**3**) as a lead, two postdoctoral fellows, Dr. Ze Li and Dr. Chamani Perera in our group designed and synthesized analogues (**7-9,** Figure 2.5) aimed to facilitate the disruption of endosomes. Fluorescence-based assays run by Mr. David Hymel in our group demonstrated that these compounds were potent endosome disruptors (Figure 2.6).

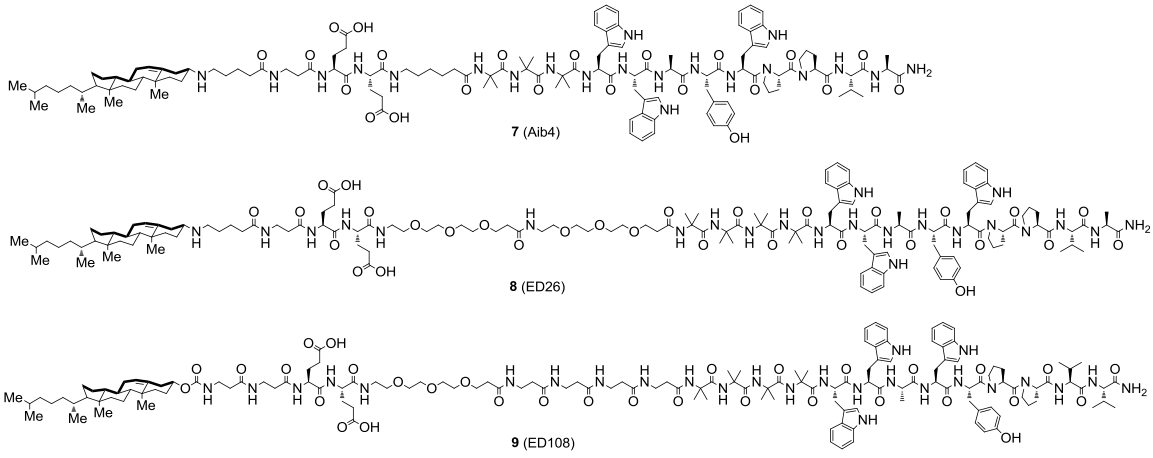

Figure **2.5**: Structures of *N*-alkyl-3β-cholesterylamine-capped peptides (**7**-**9**)

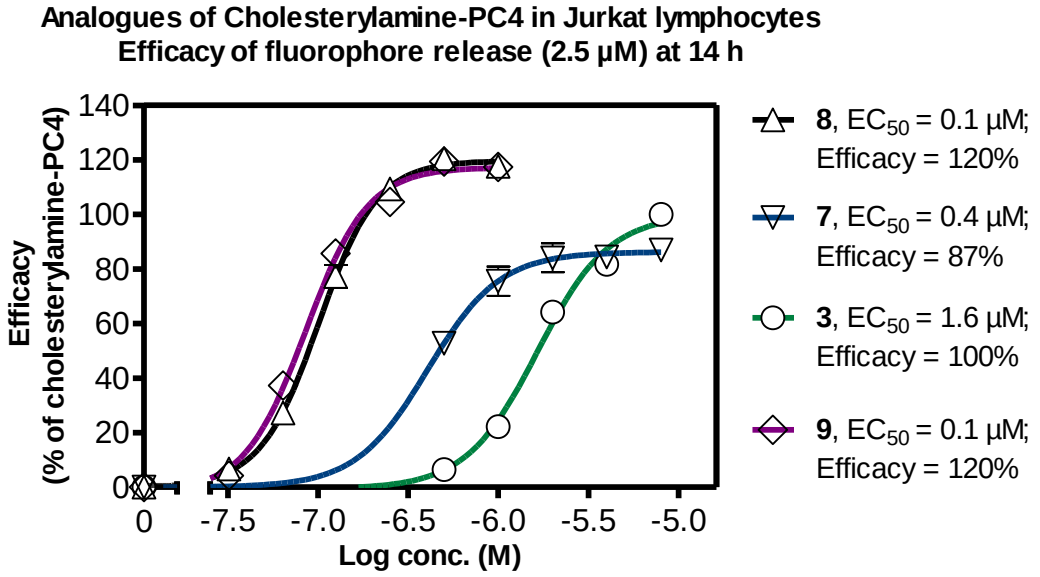

Figure **2.6**: Efficacy and potency of analogues of cholesterylamine-PC4 (**7**-**9**) in Jurkat lymphocytes. Release of fluorophore (2.5 μM) into the cytoplasm results in enhanced cellular fluorescence that was measured by flow cytometry.

Inspired by the results from fluorescence-based assays of endosome disruption, we sought to explore a potential application of our novel early/recycling endosome-targeting system for drug delivery. We describe in this chapter the synthesis of novel disulfide-linked cholesterylamine conjugates of colchicine and colchinol methyl ether designed to localize the tubulin-binding moiety in early/recycling endosomes to minimize its cytotoxic effect. Only upon the activation by an endosome disruptive peptide would the tubulin-binding moiety be released into the cytosol and kill the cells. This binary drug delivery strategy was expected to modulate the cytotoxic effect of a nonselective cytotoxin by trapping the prodrug in early/recycling endosomes. The endosome disruptive peptide would be used to release the toxic headgroup in a controlled manner (Figure 2.7).

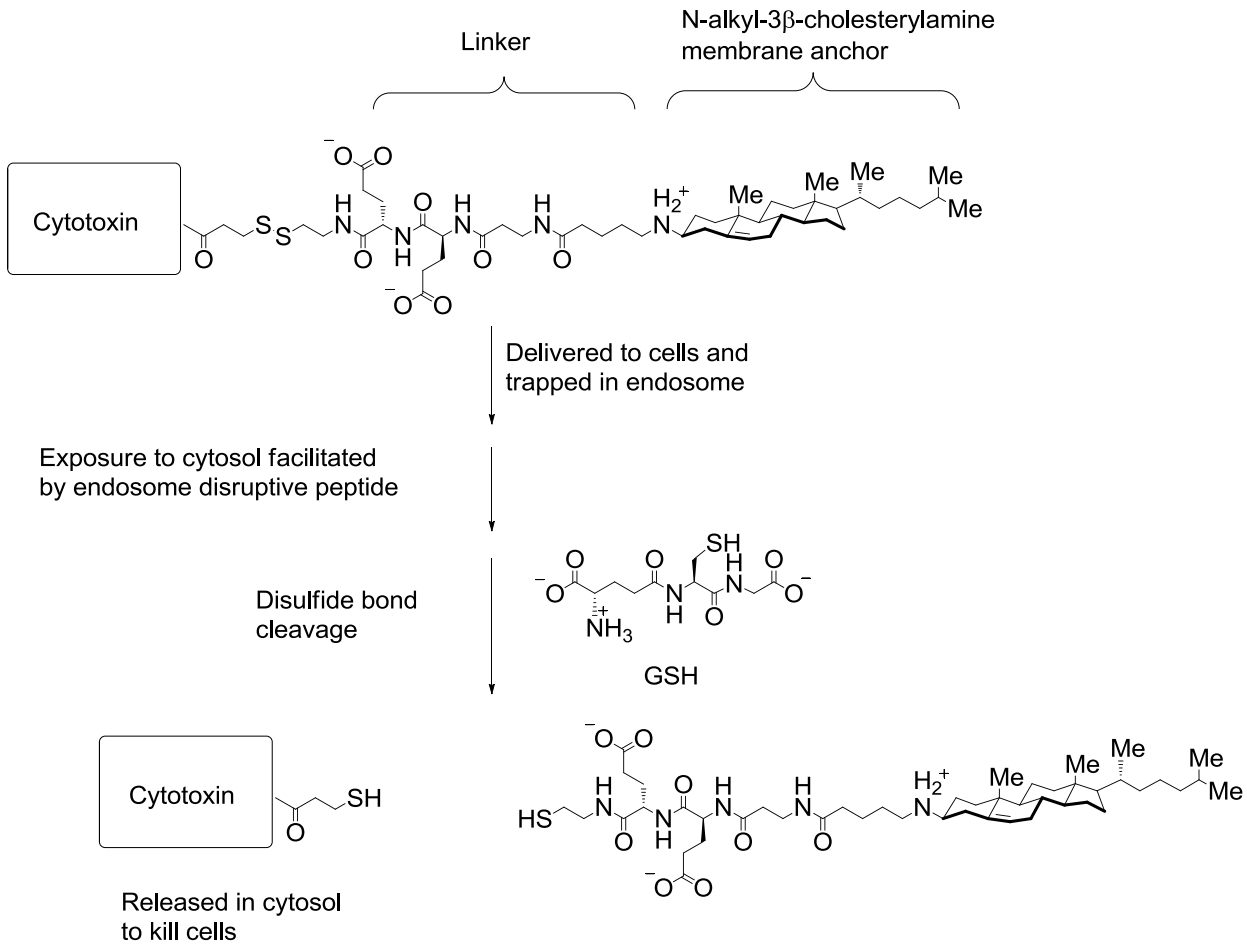

Figure **2.7**: Proposed molecular mechanism for the selective release of a disulfide-linked cytotoxin from early/recycling endosomes mediated by an endosome disruptive peptide.

2.2 Design, Synthesis, Evaluation of Disulfide-Linked Cholesterylamine Conjugates of Colchicine and Colchinol methyl ether

Deacetylcolchicine trifluoroacetate (**13**) was synthesized as previously reported in literature (Figure 2.8).[34] We designed and synthesized four derivatives of this agent linked to *N*-alkyl-3β-cholesterylamines[35, 36] (**16**-**19**, Figure 2.8). Three of these compounds (**16**, **18**, **19**) have a disulfide bond that is designed to allow cleavage by reduced glutathione. Compound **17**, prepared as a control, replaces the disulfide of **16** with a more stable amide.

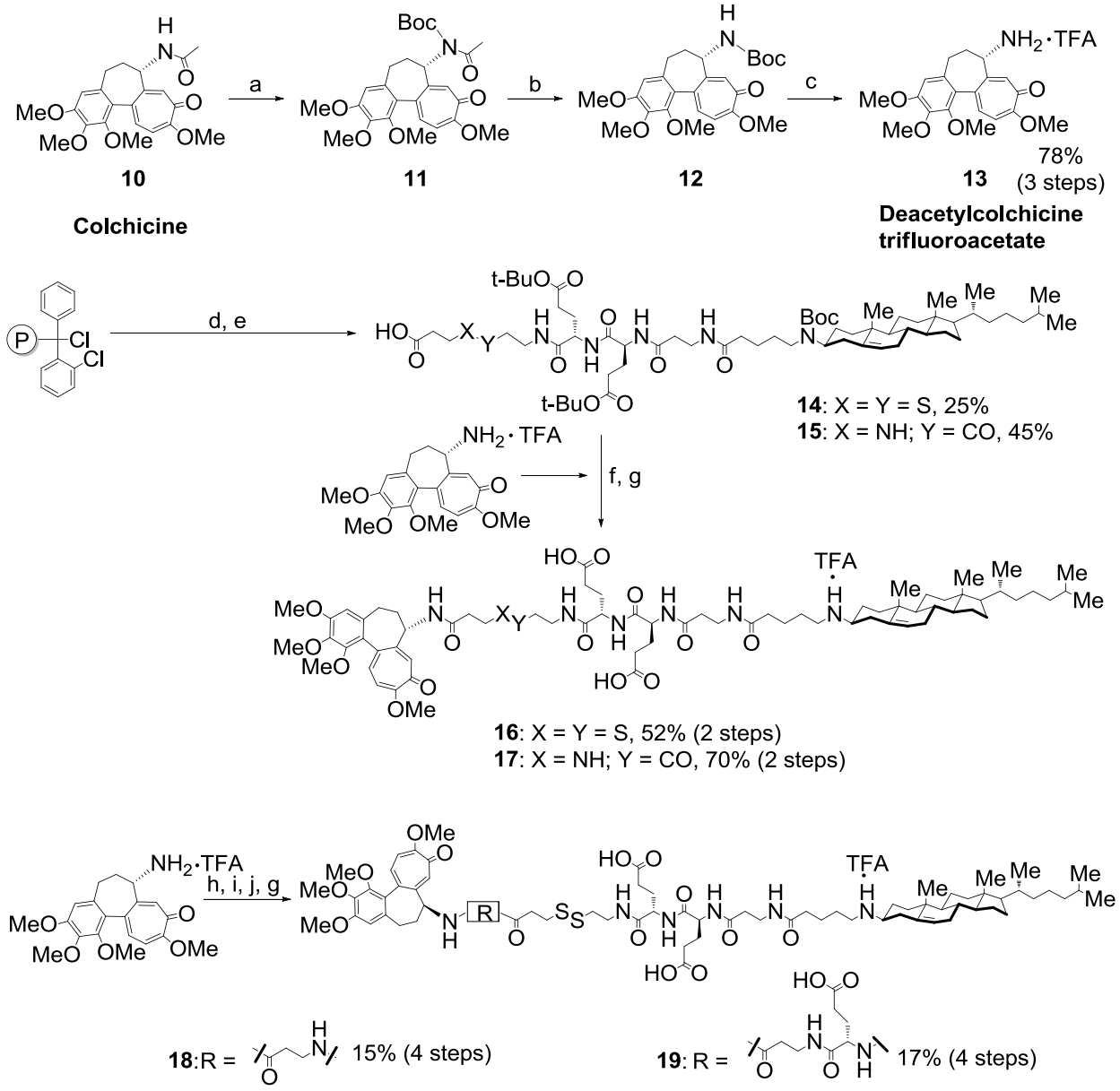

Figure **2.8**: Synthesis of deacetylcolchicine trifluoroacetate and colchicine-cholesterylamine conjugates (**16**-**19**). Reagents and conditions: (a) Boc_2O, DMAP, TEA, CH_3CN, 100 ^oC, 3 h; (b) 2M $NaOCH_3$ in CH_3OH, 22 ^oC, 1 h; (c) TFA, 22 ^oC, 5 min; (d) solid phase synthesis on 2-chlorotrityl resin; (e) cleavage from resin with acetic acid/TFE/DCM (1: 2: 7 by volume); (f) HATU, DIEA, CH_2Cl_2, 22 ^oC, 16 h; (g) TFA/CH_2Cl_2 (3: 17, by volume), 22 ^oC, 3 h; (h) Fmoc-β-Ala-OH/Fmoc-Glu(t-Bu)-β-Ala-OH, HATU, DIEA, CH_2Cl_2, 22 ^oC, 16 h; (i) Si-piperazine, DIEA, DMF, 22 ^oC, 16 h; (j) **14**, HATU, DIEA, CH_2Cl_2, 22 ^oC, 16 h.

We hypothesized that the colchicine-cholesterylamine conjugates (**16**-**19**) would cycle between the cell surface and intracellular endosomes when added to mammalian cells.

Because the partitioning of structurally similar compounds between the plasma membrane and endosomes is affected by the structure of the linker region proximal to the membrane anchor,[33] in **16**-**19**, two glutamic acid residues were installed in this region to enhance the localization of these compounds in endosomes compared to the plasma membrane. In order to explore the effect of the linker region proximal to the tubulin-binding moiety, β-alanine and β-alanine-glutamic acid were included in the linker region of **18** and **19**. Based on our previous studies of fluorescent probes, the disulfide bond of compounds (**16**, **18**, **19**) should be relatively stable in endosomes. However, we hypothesized that the endosome disruptive peptide would disrupt early/recycling endosomes loaded with **16**, **18**, or **19**, enable GSH to access these compartments, reduce the disulfide bond, and release the toxic tubulin-binding moiety to kill cells.

To investigate this concept, Jurkat lymphocytes were treated with **16**-**19** in the presence or absence of endosome disruptive peptides (Figure 2.5). As hypothesized, cell viability assays showed that the colchicine-cholesterylamine conjugate **16** (IC_{50} ~ 400 nM) reduced the toxicity of the parent compound colchicine (IC_{50} ~ 2.1 nM), consistent with the proposed mechanism of trapping the warhead in endosomes (Figure 2.9). However, the IC_{50} of **16** alone indicated that this compound still possesses some toxicity, which is likely due to slight reduction of the disulfide in endosomes during the 48 hour incubation. This interpretation is supported by the fact that control compound **17** where the disulfide is replaced with an amide was less toxic, with essentially no toxicity observed at 500 nM. These results established that the cytotoxicity of a tubulin-binding agent can be controlled by linking these molecules to the endosome-targeting N-alkyl-3β-cholesterylamine membrane anchor. On the other hand, the combination of **16** and **7** (IC_{50} ~ 50 nM), was nearly 8 fold as potent as **16** alone, indicating that activation by **7** induced the release of the colchicine-derived cytotoxin headgroup (Figure 2.9).

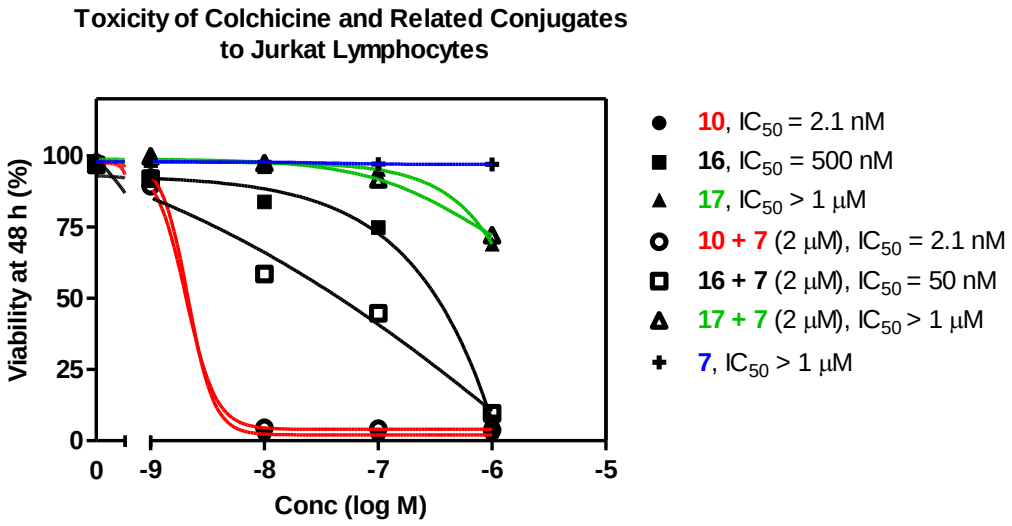

Figure **2.9**. Toxicity to Jurkat lymphocytes of **16** and controls (**10**, **17**) in the presence or absence of endosome disruptor **7** (2 μM). The viability of the cells was determined by flow cytometry after incubation with compounds (0 to 1 μM) for 48 h at 37 ^{o}C.

Compared with the parent compound colchicine, cell viability assays showed that the colchicine-cholesterylamine conjugate **18** (IC_{50} ~ 21 nM) had a 10-fold reduction in toxicity and **19** (IC_{50} ~ 56 nM) had a 25-fold reduction in toxicity (Figure 2.10). On the other hand, the combination of **18** and **7** (IC_{50} ~ 2.6 nM), was almost 8 fold as potent as **18** alone; the combination of **19** and **7** (IC_{50} ~ 2.3 nM), was nearly 25 fold as potent as **19** alone, indicating that **7** could facilitate the disruption of early endosomes and release the toxic cargo. In combination with **7**, both **18** and **19** were more potent than **16**, indicating the linker region proximal to colchicine might affect the activity of cytotoxin headgroup after the cleavage of disulfide bond. However, the estimated IC_{50} of **18** and **19** showed that these two compounds alone retained high levels of toxicity. We hypothesized that this high toxicity in the absence of **7** may relate to the high electrophilicity of seven-membered tropone ring in colchicine, which could promote off-target effects due to reaction with biomolecules. Therefore, we sought to examine another related cytotoxin with potentially better properties in this type of delivery system.

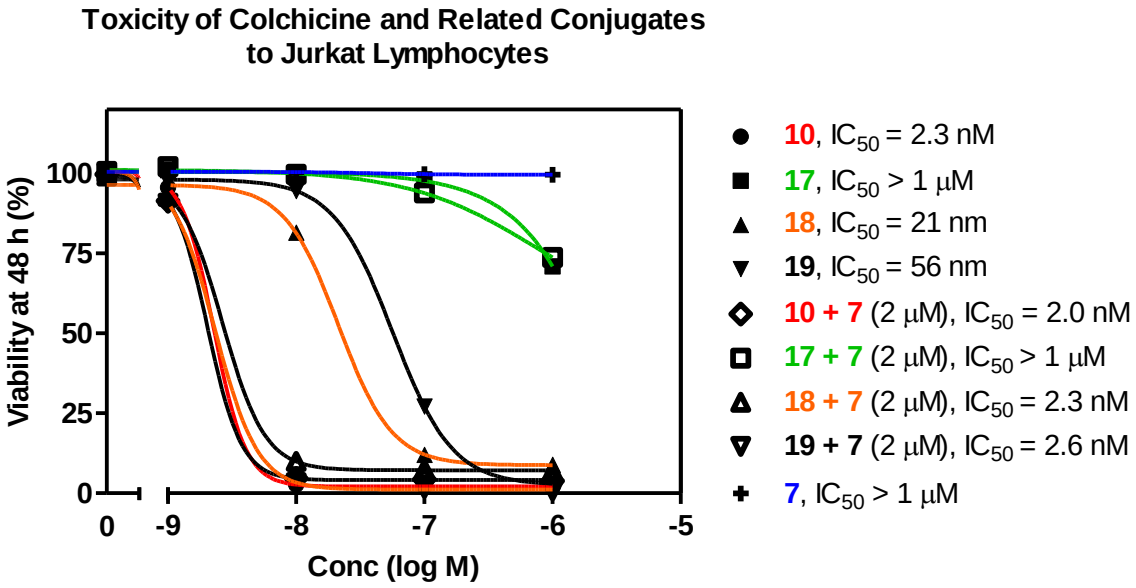

Figure **2.10**: Toxicity to Jurkat lymphocytes of compounds (**18**, **19**) and controls (**10**, **17**) in the presence or absence of **7** (2 μM). The viability of the cells was determined by flow cytometry after incubation with compounds (0 to 1 μM) for 48 h at 37 ^{o}C.

N-Acetylcolchinol methyl ether (NACM, **23**) is a potent analogue of colchicine with a methoxy-substituted benzenoid ring instead of the methoxy-substituted tropone ring (Figure 2.11).[37] Alteration of the tropone ring is known to yield agents that are more potent than colchicine both against tumor cells and as inhibitors of tubulin.[38] Deacetylcolchinol methyl ether hydrochloride (**24**) was prepared according to procedures reported in literature (Figure 2.11).[39,40] To explore our binary drug delivery system with this cytotoxin, we designed and synthesized four colchinol methyl ether derivates linked to *N*-alkyl-3β-cholesterylamine. Compounds (**25**, **27**, **28**) have a reducible disulfide bond in the linker region, whereas compound **26**, prepared as a negative control, has an amide bond at that position. Similar to the colchicine-cholesterylamine conjugates **18** and **19**, β-alanine and β-alanine-glutamic acid were separately installed to **27** and **28** to study the effects of the linker region proximal to the colchinol methyl ether (Figure 2.11).

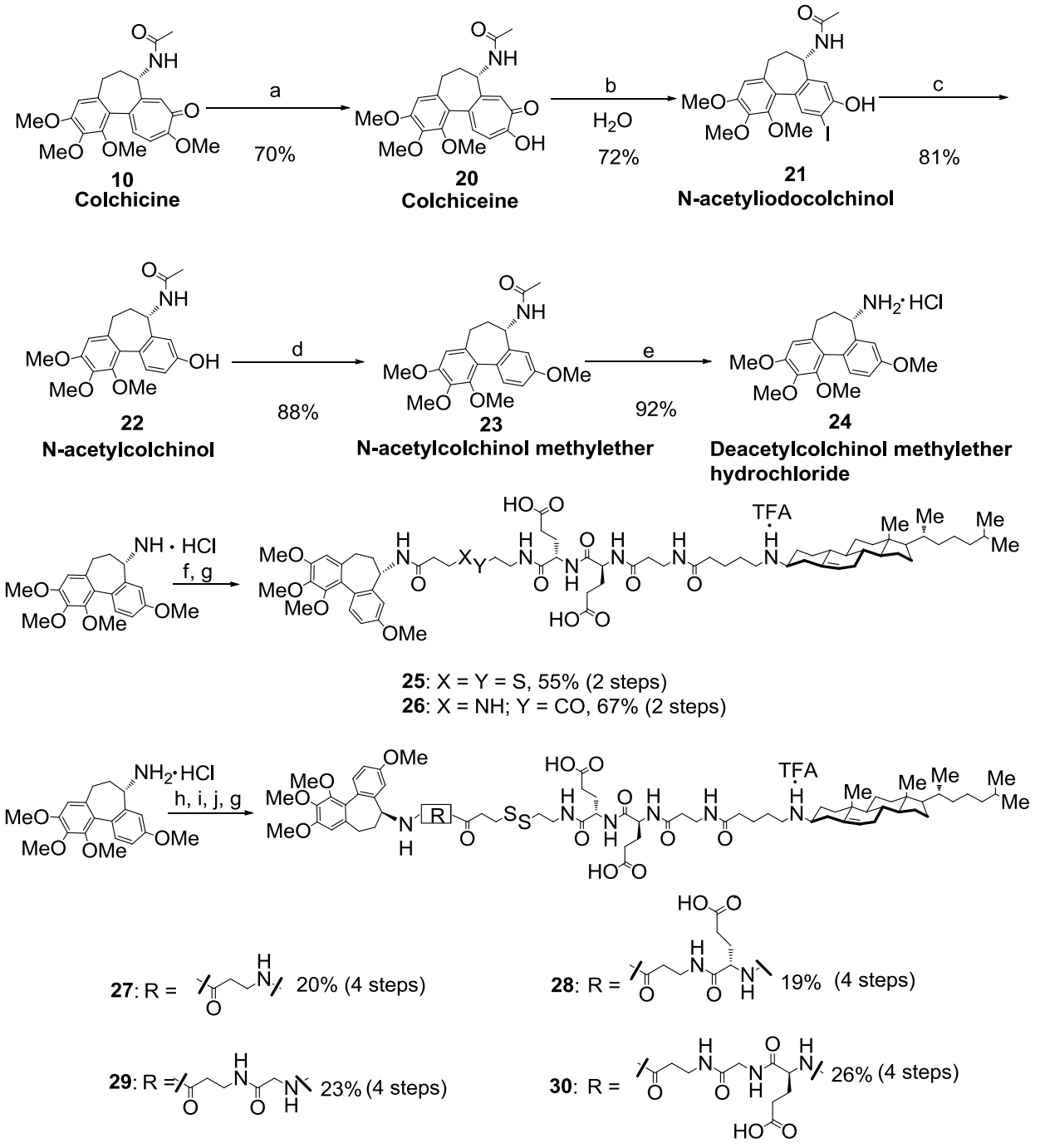

Figure **2.11**: Synthesis of deacetylcolchinol methyl ether hydrochloride and colchinol methyl ether-cholesterylamine conjugates (**25**-**30**). Reagents and conditions: (a) 0.1 N HCl, HOAc, 100 ^{o}C, 2 h; (b) NaOH, I_2, NaI, H_2O, 22 ^{o}C, 3 h; (c) Zn, HOAc, 100 ^{o}C; (d) MeI, K_2CO_3, acetone, 56 ^{o}C; (e) 2N HCl, MeOH, 90 ^{o}C; (f) **14**/**15**, EDC, HOBt, CH_2Cl_2, 22 ^{o}C, 16 h; (g) TFA/CH_2Cl_2 (3: 17, by volume), 22 ^{o}C, 3 h; (h) Fmoc-β-Ala-OH/Fmoc-Glu(t-Bu)-β-Ala-OH/Fmoc-Gly-β-Ala-OH//Fmoc-Glu(t-Bu)-Gly-β-Ala-OH, EDC, HOBt, CH_2Cl_2, 22 ^{o}C, 16 h; (i) Si-piperazine, DIEA, DMF, 22 ^{o}C, 16 h; (j) **14**, HATU, DIEA, CH_2Cl_2, 22 ^{o}C, 16 h.

Flow cytometry-based cell viability assays showed the IC_{50} values of colchinol methyl ether-cholesterylamine conjugates (**25**, **27**, **28**) were greater than 1 μM (Figure 2.12, Panel A), suggesting that the toxicity of the parent compound colchinol methyl ether was significantly reduced by trapping the warhead in endosomes. On the other hand, the combination of **28** and endosome disruptor **7** (IC_{50} ~ 110 nM, Figure 2.12, Panel B), was over 9 times more potent than **28** alone. However, in combination with **7**, both **25** and **27** did not differ substantially in their potency, indicating that the linker region proximal to the colchinol methyl ether strongly affects the activity of cytotoxin headgroup. In an additional set of experiments, we investigated how a more potent endosome disruptive peptide (**8**) would affect the cytotoxicity of compounds (**25**-**28**). Similar to the previous results, only the combination of **28** and **8** (IC_{50} ~ 150 nM) showed high potency (Figure 2.12, Panel C), indicating that the β-alanine-glutamic acid sequence is beneficial for improving the potency of colchinol methyl ether-cholesterylamine conjugate.

To further investigate the effect of the linker region proximal to colchinol methyl ether on the potency of colchinol methyl ether-cholesterylamine conjugate, two other compounds (**29**, **30**) were designed and synthesized (Figure 2.11). Compared with **28**, the glutamic acid in the linker region was replaced by glycine in **29**, and **30** has one additional glycine between the β-alanine and glutamic acid.

Both **29** and **30** were essentially non-toxic to Jurkat lymphocytes at a concentration of 1 μM (Figure 2.13). In combination with **8**, the potency of compound **30** (IC_{50} ~ 27 nM) was increased by over 35 fold, but compound **29** did not show enhanced potency (Figure 2.13).

A. Toxicity of NACM (**23**) and Related Conjugates to Jurkat Lymphocytes

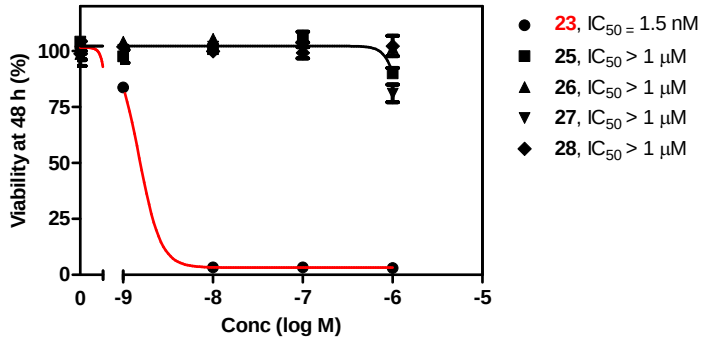

B. Toxicity of NACM (**23**) and Related Conjugates to Jurkat Lymphocytes (with **7** at 2 µM)

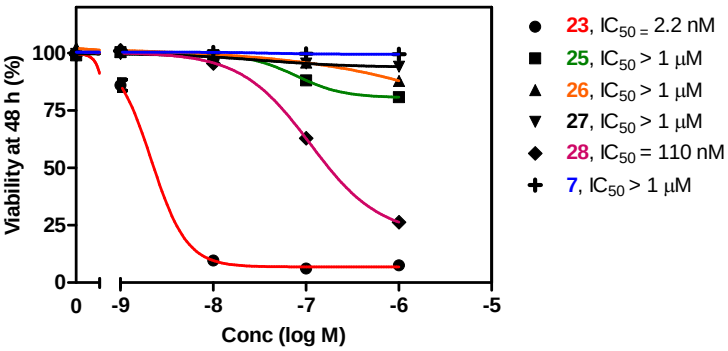

C. Toxicity of NACM (**23**) and Related Conjugates to Jurkat Lymphocytes (with **8** at 100 nM)

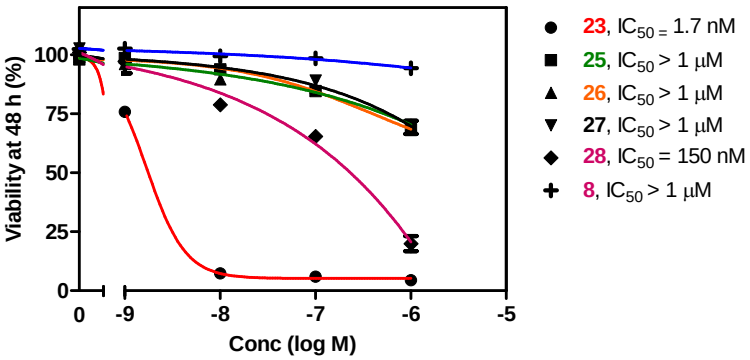

Figure **2.12**: Toxicity to Jurkat lymphocytes of compounds (**25**, **27**, **28**) and controls (**23**, **26**) in the absence or presence of endosome disruptor **7** or **8**. Panel A: Toxicity to Jurkat lymphocytes. Panel B: Toxicity to Jurkat lymphocytes in the presence of **7** (2 µM). Panel C: Toxicity to Jurkat lymphocytes in the presence of **8** (100 nM). The viability of the cells was determined by flow cytometry based assay after incubation with compounds (0 to 1 µM) for 48 h at 37 ^{o}C.

This result, together with the previous study of **28**, demonstrated that the glutamic acid in the linker region was important for maintaining the potency of colchinol methyl ether-cholesterylamine conjugates in the presence of the endosome disruptive peptide.

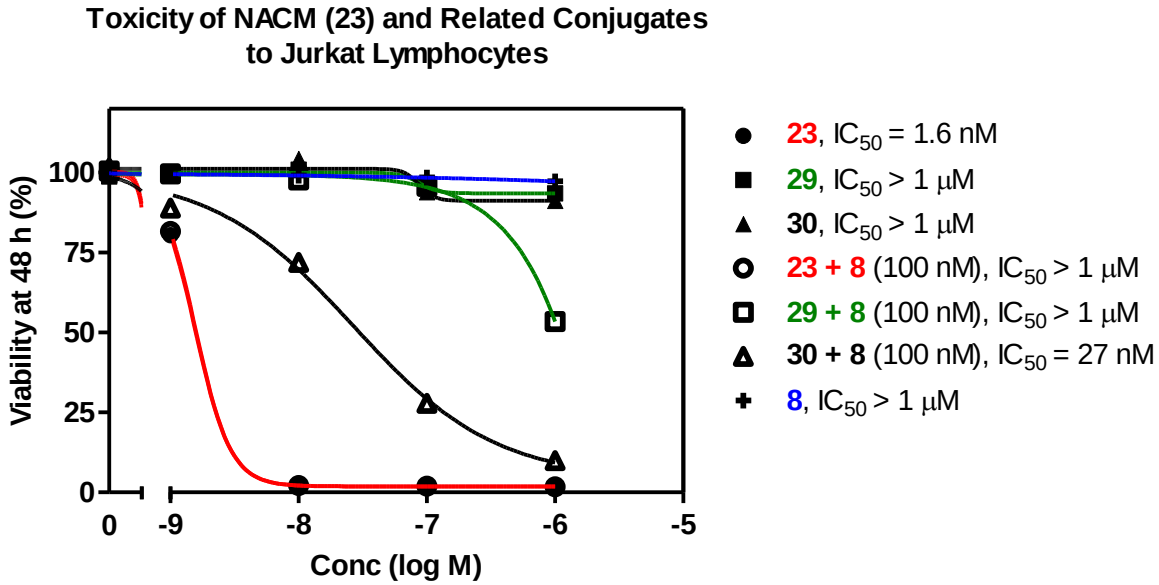

Figure **2.13**: Toxicity to Jurkat lymphocytes of compounds (**29**, **30**) and controls (**23**) in the presence or absence of endosome disruptor **8** (100 nM). The viability of the cells was determined by flow cytometry after incubation with compounds (0 to 1 μM) for 48 h at 37 ^{o}C.

As described previously, the *N*-alkyl-3β-cholesterylamine derived drug delivery system was able to reduce the toxicity of the parent compound colchinol methyl ether, and in combination with endosome disruptive peptides, some colchinol methyl ether-cholesterylamine conjugates showed good potency against the proliferation of Jurkat lymphocytes. Based on these results, we decided to study whether our binary delivery system might be effective in other cancer cell lines, PC3, DU145 and A549. PC3 and DU145 are human prostate cancer cell lines. These cells are useful in investigating the biochemical changes in advanced prostatic cancer cells and in assessing their response to chemotherapeutic agents.[41] DU145 cells have moderate metastatic potential compared to PC3 cells which have high metastatic potential.[42] A549 cells are adenocarcinomic human alveolar basal epithelial cells. These cells can be used for evaluation of chemotherapy agents against lung cancer.[43]

We designed and synthesized two additional colchinol methyl ether-cholesterylamine conjugates (**31**, **33**) for exploring a potential application of our binary delivery system in different cancer cell lines. Compound **31** has a β-alanine-β-alanine-glutamic acid sequence in the linker region proximal to colchinol methyl ether and **33** was prepared as a negative control with an amide bond replacing the disulfide bond (Figure 2.14).

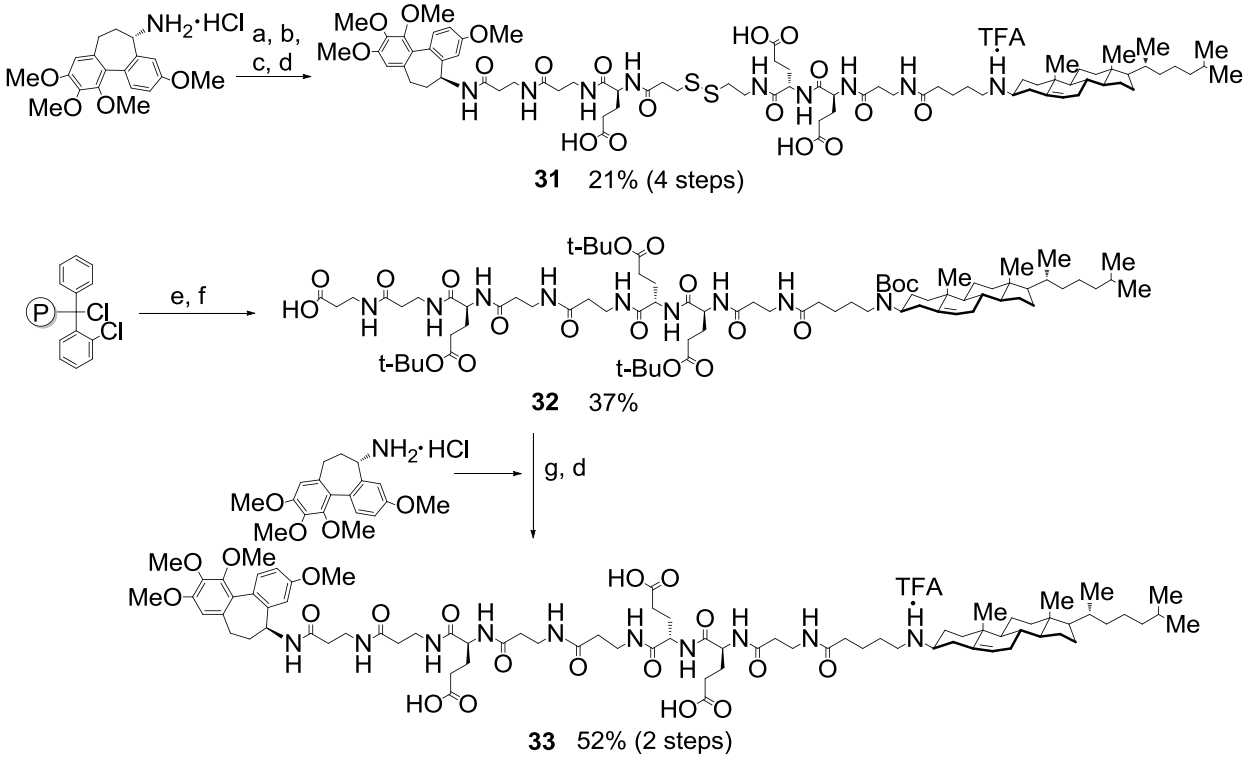

Figure **2.14**. Synthesis of colchinol methyl ether-cholesterylamine conjugates (**31**, **33**). Reagents and conditions: (a) Fmoc-Glu(t-Bu)-β-Ala-β-Ala-OH, EDC, HOBt, CH_2Cl_2, 22 ^oC, 16 h; (b) Si-piperazine, DIEA, DMF, 22 ^oC, 16 h; (c) **14**, HATU, DIEA, CH_2Cl_2, 22 ^oC, 16 h; (d) TFA/CH_2Cl_2 (3: 17, by volume), 22 ^oC, 3 h; (e) solid phase synthesis on 2-chlorotrityl resin; (f) cleavage from resin with acetic acid/TFE/DCM (1: 2: 7 by volume); (g) HATU, DIEA, CH_2Cl_2, 22 ^oC, 16 h.

Flow cytometry-based cell viability assays were employed to study the toxicities of **31** and **33** in Jurkat lymphocytes, PC3 cells, DU145 cells and A549 cells. The endosome disruptive peptide **9** (Figure 2.5) was used to facilitate the release of the cytotoxin. In Jurkat lymphocytes, the combination of **31** and **9** (IC_{50} ~ 36 nM) was over 25 fold more potent than **31** alone (Figure 2.15, Panel A). Also in combination with **9**, the potency of **31** (IC_{50} ~ 112 nM) to inhibit the

A. Toxicity of NACM (**23**) and Related Conjugates to Jurkat Lymphocytes

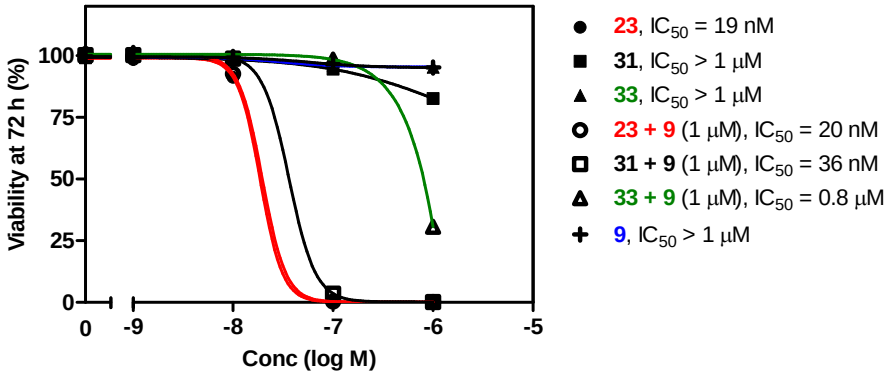

B. Toxicity of NACM (**23**) and Related Conjugates to PC3 cells

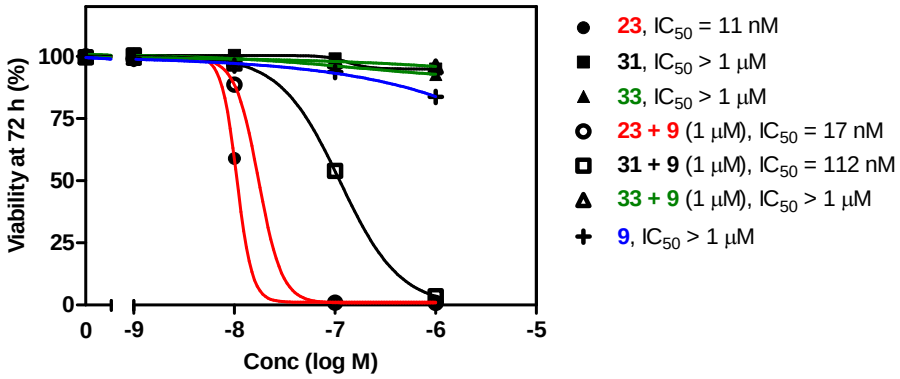

C. Toxicity of NACM (**23**) and Related Conjugates to DU145 cells

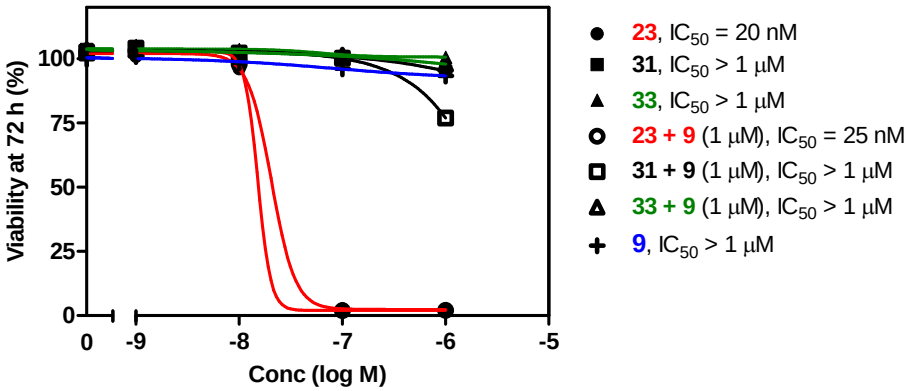

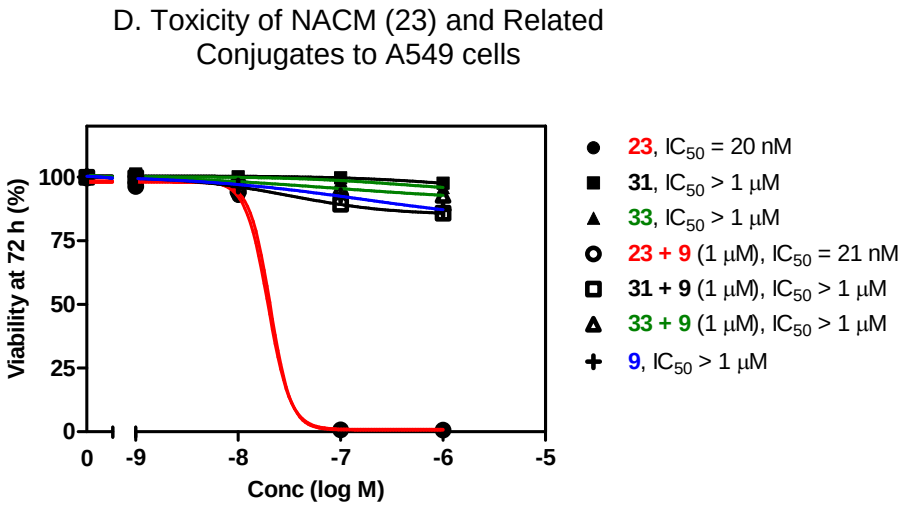

Figure **2.15**: Toxicity to four cancer cell lines of **31** and controls (**23**, **33**) in the presence or absence of endosome disruptor **9** (1 μM). Panel A: Toxicity to Jurkat lymphocytes. Panel B: Toxicity to PC3 cells. Panel C: Toxicity to DU145 cells. Panel D: Toxicity to A549 cells. The viability of the cells was determined by flow cytometry after incubation with compounds (0 to 1 μM) for 48 h at 37 ^{o}C.

proliferation of PC3 cells was increased by over 9 fold (Figure 2.15, Panel B). However, compared with **31** alone the potency of **31** in DU145 and A549 cells was not enhanced in combination with **9** (Figure 2.15, Panel C and Panel D). These results showed that our binary delivery system was effective for delivering cytotoxins into some types of cancer cells, however, some other cancer cell lines appear to be less sensitive to this delivery system.

2.3 Conclusions

In summary, a major challenge associated with cancer chemotherapy is the low therapeutic index of many cytotoxic agents, including tubulin binding agents. As a strategy to modulate the cytotoxic effect of a tubulin binding agent, we designed and synthesized disulfide-linked colchicine and colchinol methyl ether derivatives linked to the membrane anchor *N*-alkyl-3β-cholesterylamine to selectively localize these compounds in early/recycling endosomes. Cell viability assays indicated that the cytotoxic effect of colchinol methyl ether could be diminished

by trapping the molecule in sealed endocytic vesicles and reactivated by disrupting the endosomes with the endosome disruptive peptide to release a thiol derivative. The linker region proximal to the colchinol methyl ether was found to strongly affect the activity of the cytotoxin. Comparison of the toxicities of colchinol methyl ether-cholesterylamine conjugates (**25**-**30**, **31**, **33**) in the presence of an endosome disruptive peptide demonstrated that insertion of a glutamic acid residue in the linker region was able to significantly increase the potency. This negatively charged glutamic acid residue may improve activity by minimizing efflux of the colchinol methyl ether warhead crossing the plasma membrane, consequently enhancing its accumulation in the cytosol. This binary cytotoxin delivery system was demonstrated to be effective in inhibiting the proliferation of Jurkat lymphocytes and PC3 cells, but other cancer cell lines such as DU145 and A549 cells were much less sensitive. We hypothesize that DU145 cells and A549 cells may express drug efflux pumps that decrease levels of the intracellular cytotoxin or the endosome disruptive peptides may show lower efficacy in these cell lines for unknown reasons.

2.4 Future directions

The success of chemotherapy can be limited by insufficient drug concentrations in tumors, systemic toxicity, a lack of selectivity for tumor cells over normal cells, and the appearance of drug-resistant tumor cells.[44-46] One promising area for improving tumor selectivity is tumor-enzyme activated chemotherapy.[47] Tumor-enzyme activated chemotherapy is usually a two-step approach. In the first step, a drug-activating enzyme over expressed by tumors is identified. In the second step, a nontoxic prodrug, a substrate of this enzyme, is administered systemically.[44, 45] The net gain is that a systemically administered prodrug can be converted into a high local concentration of an active anticancer drug in tumors. Tumor-enzyme activated chemotherapy shows particular promise for targeting membrane-type matrix metalloproteinases (MT-MMPs) for activation of anticancer agents. MT-MMPs function to break down the

extracellular matrix to facilitate tumor invasion and also play a major role in controlling tumor cell growth, migration, differentiation, and ultimately metastasis.[48] ICT2588, a non-toxic peptide-conjugated colchiceinamide, was shown to be selectively metabolized by MT-MMPs, particularly membrane-type 1 matrix metalloproteinases (MT1-MMP), to release the active agent in the tumor (Figure 2.16)[49, 50].Importantly, significant growth delay of human fibrosarcoma HT1080 xenografts without associated systemic toxicity was observed.[49]

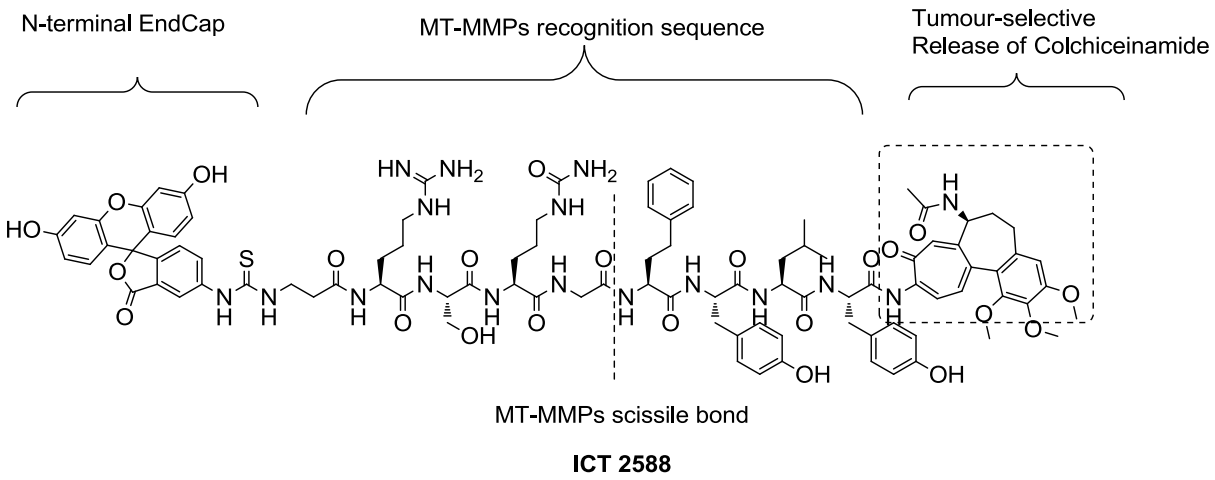

Figure **2.16**: Structure of ICT2588, a compound shown to be selectively cleaved by MT-MMPs to release colchiceinamide

Inspired by the results from this research, we sought to design and synthesize peptides that can be selectively metabolized by MT-MMPs expressed in tumor to release an active endosome disruptive peptide. The activation of the endosome disruptive peptide selectively in the tumor, coupled with colchinol methyl ether-cholesterylamine conjugates, might lead to significant antitumor effect with a greater therapeutic index. These studies are currently underway.

Aptamers are oligonucleotides or peptides capable of specific and tight binding to their target. Several unique properties of aptamers make them attractive tools for use in targeted drug delivery. The advantages of aptamers over other drug delivery system include high binding affinity, greater stability, ease of synthesis, and lower production cost.[51] The possible targets of

aptamers can exhibit great diversity ranging from small molecules to proteins and whole cells.[52,53] One important class of targets for aptamers is cell surface receptors. Most cell surface proteins cycle intracellularly to some extent, and many surface receptors are actively internalized in response to ligand binding.[54] Therefore, aptamers that bind cell surface receptors have been exploited for the delivery of a variety of cargoes into cells.[55] In future research, we are planning to investigate whether aptamers might be useful for targeting cell surface receptors and delivery of endosome disruptive peptides and cytotoxins. One cell surface receptor of interest is the prostate-specific membrane antigen (PSMA), a type 2 integral membrane glycoprotein expressed on the surface of prostate carcinoma and the neovasculature of most other solid tumors. The antigen is abundantly expressed at all stages of the cancer and is therefore an attractive target for cancer immunotherapy and imaging.[56.57]

In addition to aptamers and antibodies, small molecules can be used to target some cell surface receptors. For example, Professor Philip Low and coworkers conducted *in silico* docking studies and identified 2-[3-(1, 3-dicarboxypropyl)-ureido]pentanedioic acid (DUPA) as a ligand of PSMA with high affinity.[58]

Inspired by the results from this research, the construction of a DUPA based delivery system (Figure 2.17), designed to selectively transport probes or cytotoxins into the prostate cancer cells through the binding of DUPA with PSMA, is currently underway. Combined with endosome disruptive peptides, this approach may enhance therapeutic index of anticancer agents.

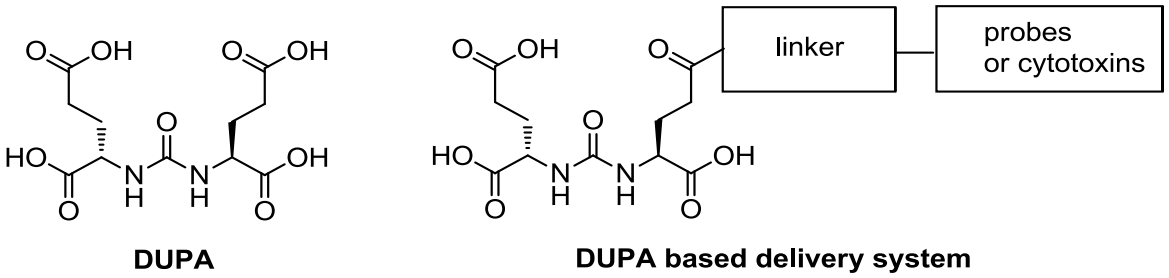

Figure **2.17**: Structure of DUPA and proposed DUPA based delivery system.

2.5 Experimental Section

2.5.1 General

Chemical reagents were obtained from Sigma Aldrich, TCI, or Alfa Aesar. Solvents were from Sigma Aldrich or Fisher Sci. Commercial grade reagents were used without further purification unless otherwise noted. Detailed synthetic procedures and characterization data of deacetylcolchicine trifluoroacetate (**13**) and deacetylcolchinol methyl ether hydrochloride (**24**) have been previously described.[34, 39, 40] Compound **7** was prepared by Dr. Ze Li, a former postdoctoral fellow in the Peterson laboratory. Compounds **8** and **9** were prepared by Dr. Chamani Perera of the Peterson laboratory. Anhydrous solvents were obtained after passage through a drying column of a solvent purification system from GlassContour (Laguna Beach, CA). All reactions were performed under an atmosphere of dry nitrogen. Reactions were monitored by analytical thin-layer chromatography on plates coated with 0.25 mm silica gel 60 F254 (EMD Chemicals). TLC plates were visualized by UV irradiation (254 nm) or stained with a solution of phosphomolybdic acid in ethanol (20%). Flash column chromatography employed ICN SiliTech Silica Gel (32-63 μm). Purification by preparative reverse phase HPLC employed an Agilent 1200 preparative pump/gradient extension instrument equipped with a Hamilton PRP-1 (polystyrene-divinylbenzene) reverse phase column (7 μm particle size, 21.5 mm × 25 cm). The HPLC flow rate was maintained at 25 mL/min for the entire run unless otherwise noted. NMR spectra were obtained with Bruker DRX-400 instruments with chemical shifts reported in parts per million (ppm, δ) referenced to either $CDCl_3$ (^{1}H 7.27 ppm; ^{13}C 77.2 ppm), MeOH-d_4 (^{1}H 4.80 ppm; ^{13}C 49.2 ppm), DMSO-d_6 (^{1}H 2.50 ppm; ^{13}C 39.5 ppm), or $(CH_3)_4Si$ (0 ppm). Low-resolution mass spectra were obtained from Waters Micromass ZQ Mass Spectrometer. Peaks are reported as *m/z*.

2.5.2 Synthetic Procedures and Compound Characterization Data

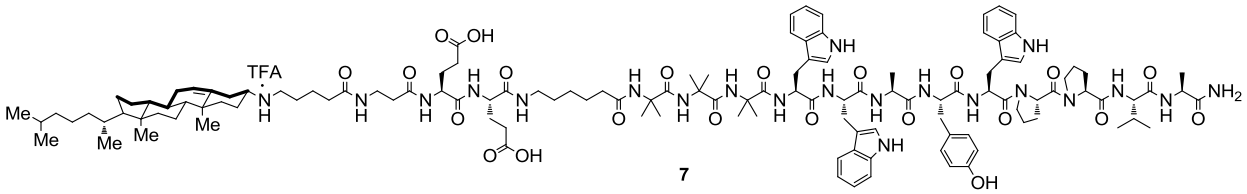

7

LRMS (ESI+) *m/z* 2339.2 ($M+H^+$, $C_{126}H_{79}N_{21}O_{22}$ requires 2339.4).

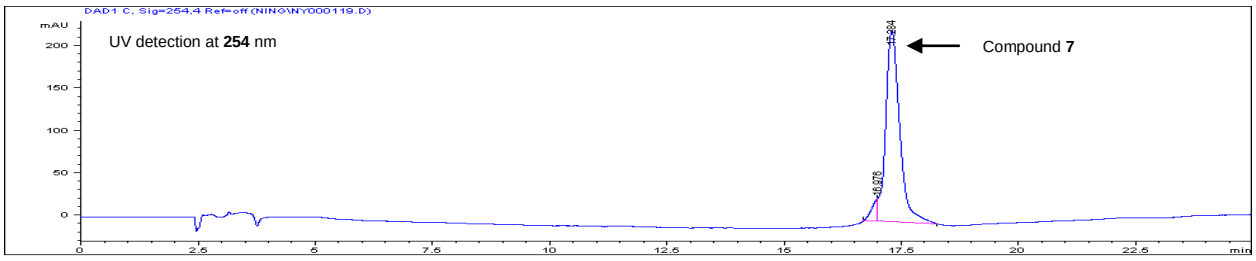

Figure **2.18**: Analytical HPLC profile of compound **7** after purification by preparative HPLC. Retention time = 17.2 min. Purity by HPLC > 95%.

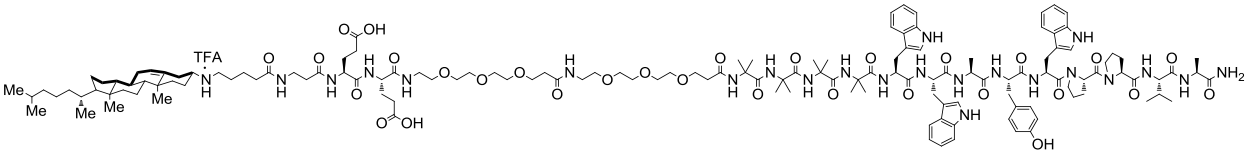

8

LRMS (ESI+) *m/z* 2717.7 ($M+H^+$, $C_{142}H_{209}N_{23}O_{30}$ requires 2717.6).

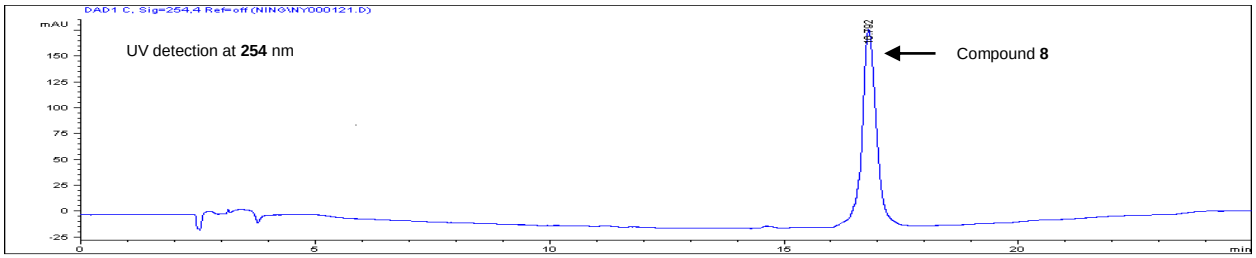

Figure **2.19**: Analytical HPLC profile of compound **8** after purification by preparative HPLC. Retention time = 16.7 min. Purity by HPLC > 99%.

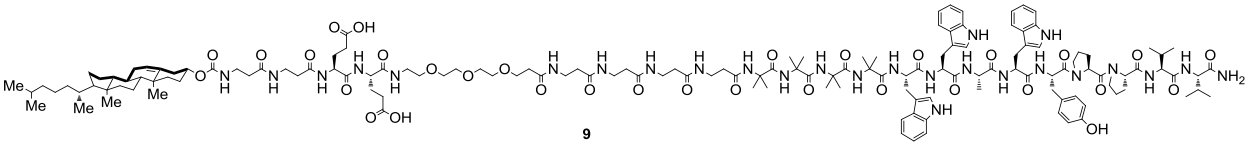

9

LRMS (ESI+) *m/z* 2842.9 ($M+H^-$, $C_{146}H_{212}N_{26}O_{32}$ requires 2842.6).

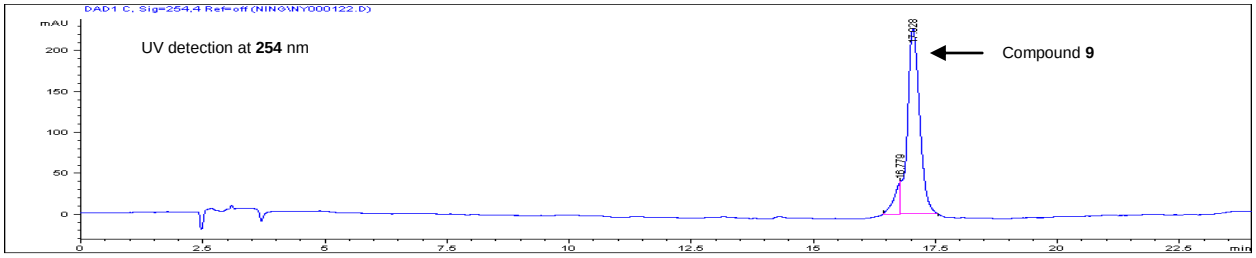

Figure **2.20**: Analytical HPLC profile of compound **9** after purification by preparative HPLC. Retention time = 17.0 min. Purity by HPLC > 95%.

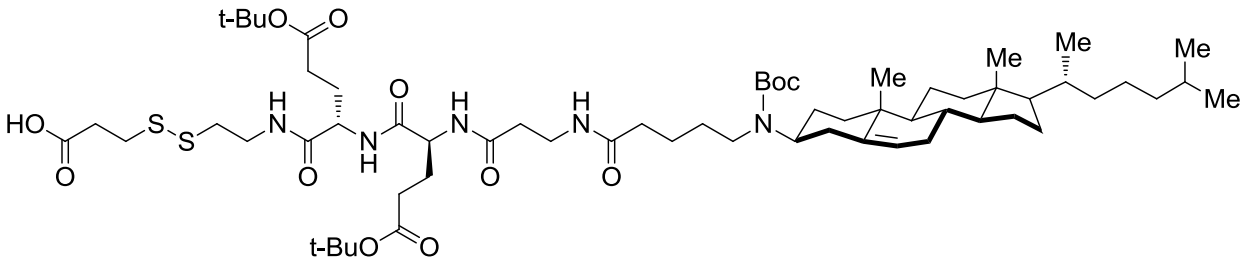

14

(16S,19S)-16,19-bis(3-(tert-butoxy)-3-oxopropyl)-5-((3S,8S,9S,10R,13R,14S,17R)-10,13-dimethyl-17-((R)-6-methylheptan-2-yl)-2,3,4,7,8,9,10,11,12,13,14,15,16,17-tetradecahydro-1H-cyclopenta[a]phenanthren-3-yl)-2,2-dimethyl-4,10,14,17,20-pentaoxo-3-oxa-24,25-dithia-5,11,15,18,21-pentaazaoctacosan-28-oic acid (14). Peptide synthesis employed a Bohdan-2080 MiniBlock and standard N-Fmoc methodology. The peptide was constructed with 2-Chlorotrityl resin (1.04 mmol/g, 96 mg, 0.1 mmol) using 5-{(tert-butoxycarbonyl) [(3β)-cholest-5-en-3yl]amino}pentanoic acid,[25] Fmoc-protected 3-((2-aminoethyl)disulfanyl)propanoic acid and the following Fmoc-protected amino acids: Fmoc-β-Ala-OH, Fmoc-Glu(t-Bu)-OH. Amino acids were consecutively coupled to the resin by addition of DMF solution (2 mL) of amino acid (4.0 eq.), HATU (3.8 eq.) and DIEA (8.0 eq.) with shaking at 22 ^{o}C for 2 h. Deprotection of Fmoc carbamates on the resin was carried out by addition of piperidine (20%) in DMF (2 mL for 5 min

followed by 2 mL for 3 min followed by 2mL for 2 min (×2)). After completing all the steps of coupling reactions, the peptide was cleaved from the resin by treatment with TFA/TFE/CH_2Cl_2 (1:2:7) with shaking for 2 h. The resin was removed by filtration and washed with CH_2Cl_2 (2 mL ×3). The filtrates were combined and concentrated *in vacuo*. The crude product was dissolved in MeOH (1 mL) and purified by preparative reverse-phase HPLC (gradient: 89.95% H_2O, 9.95% MeCN, and 0.1 % TFA to 99.9% MeCN and 0.1% TFA over 10 min; retention time = 21.0 min (214 nm)) to afford **14** as a white solid (30 mg, 25%). LRMS (ESI+) *m/z* 1190.0 ($M+H^+$, $C_{63}H_{107}N_5O_{12}S_2$ requires 1190.7).

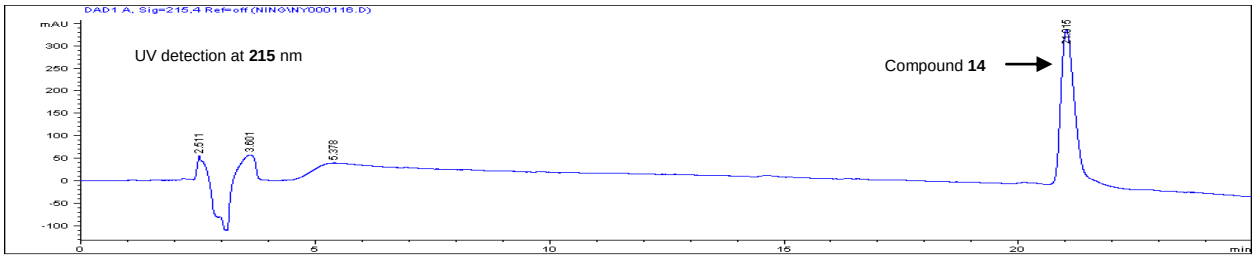

Figure **2.21**: Analytical HPLC profile of compound **14** after purification by preparative HPLC. Retention time = 21.0 min. Purity by HPLC > 99%.

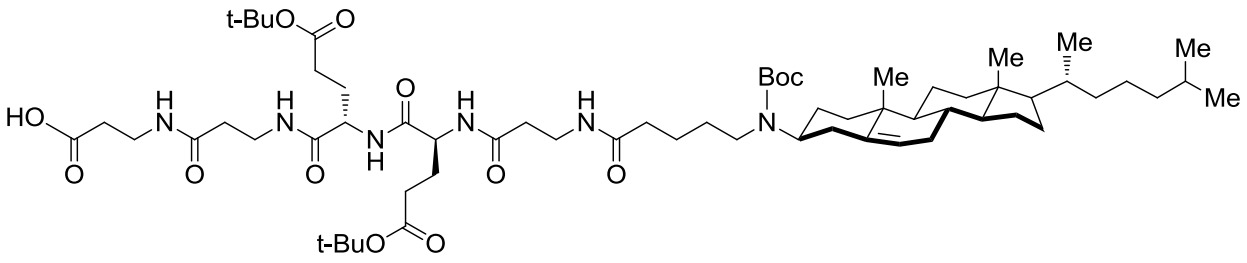

15

(16S,19S)-16,19-bis(3-(tert-butoxy)-3-oxopropyl)-5-((3S,8S,9S,10R,13R,14S,17R)-10,13-dimethyl-17-((R)-6-methylheptan-2-yl)-2,3,4,7,8,9,10,11,12,13,14,15,16,17-tetradecahydro-1H-cyclopenta[a]phenanthren-3-yl)-2,2-dimethyl-4,10,14,17,20,24-hexaoxo-3-oxa-5,11,15,18,21,25-hexaazaoctacosan-28-oic acid (15). Peptide **15** was constructed on 2-Chlorotrityl resin (1.04 mmol/g, 96 mg, 0.1 mmol) using the method described for preparation of peptide **14**. After completing all the steps of coupling reactions, the product was cleaved from

the resin with TFA/TFE/CH_2Cl_2 (1:2:7) by shaking for 2 h and purified by preparative reverse-phase HPLC (gradient: 89.95% H_2O, 9.95% MeCN, and 0.1 % TFA to 99.9% MeCN and 0.1% TFA over 10 min; retention time = 20.0 min (214 nm)) to afford **15** as a white solid (52 mg, 45%). LRMS (ESI-) *m/z* 1169.3 ($M+H^-$, $C_{64}H_{108}N_6O_{13}$ requires 1169.6).

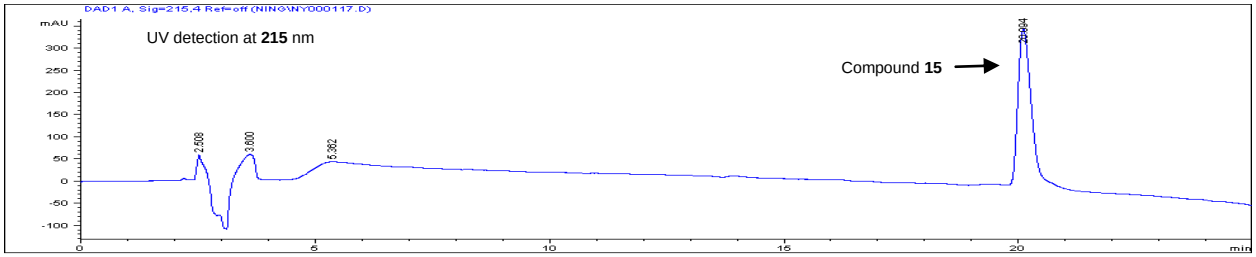

Figure **2.22**: Analytical HPLC profile of compound **15** after purification by preparative HPLC. Retention time = 20.0 min. Purity by HPLC > 99%.

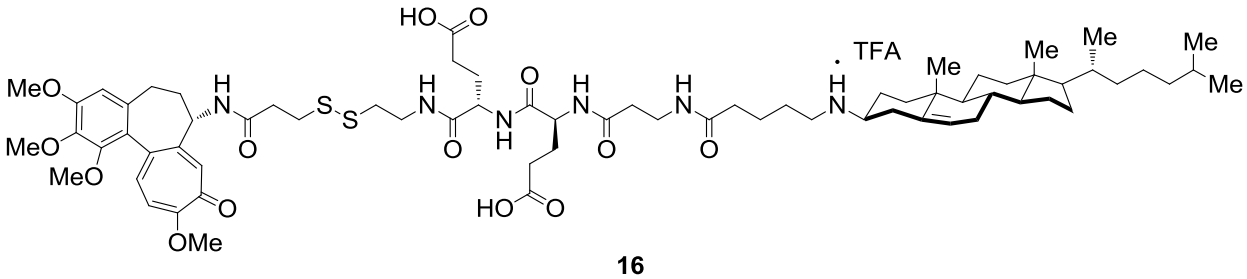

16

(S)-5-(((S)-4-carboxy-1-oxo-1-((2-((3-oxo-3-(((S)-1,2,3,10-tetramethoxy-9-oxo-5,6,7,9-tetrahydrobenzo[a]heptalen-7-yl)amino)propyl)disulfanyl)ethyl)amino)butan-2-yl)amino)-4-(3-(5-(((3S,8S,9S,10R,13R,14S,17R)-10,13-dimethyl-17-((R)-6-methylheptan-2-yl) 2,3,4,7,8,9,10,11,12,13,14,15,16,17-tetradecahydro-1H-cyclopenta[a]phenanthren-3-yl)amino)pentanamido)propanamido)-5-oxopentanoic acid (16). 13 (9 mg, 0.025 mmol) was dissolved in anhydrous CH_2Cl_2 (1 mL). To a solution of **14** (36 mg, 0.03 mmol) were added HATU (14 mg, 0.037 mmol) and DIEA (13 mg, 0.1 mmol). After 30 min, the CH_2Cl_2 solution of deacetylcolchicine was added. The reaction was stirred for 16 h at 22 ^oC and then was

concentrated *in vacuo*. The residue was dissolved in CH_2Cl_2 (5 mL) containing TFA (15%) and stirred for 3 h at 22 ^oC. The reaction was concentrated *in vacuo,* and the crude product was purified by preparative reverse-phase HPLC (gradient: 89.95% H_2O, 9.95% MeCN, and 0.1 % TFA to 99.9% MeCN and 0.1% TFA over 20 min; retention time = 18.3 min (254 nm)), which afforded **16** (17 mg, 52%) as an off white solid. LRMS (ESI-) *m/z* 1317.6 ($M+H^-$, $C_{70}H_{103}N_6O_{14}S_2$ requires 1317.7).

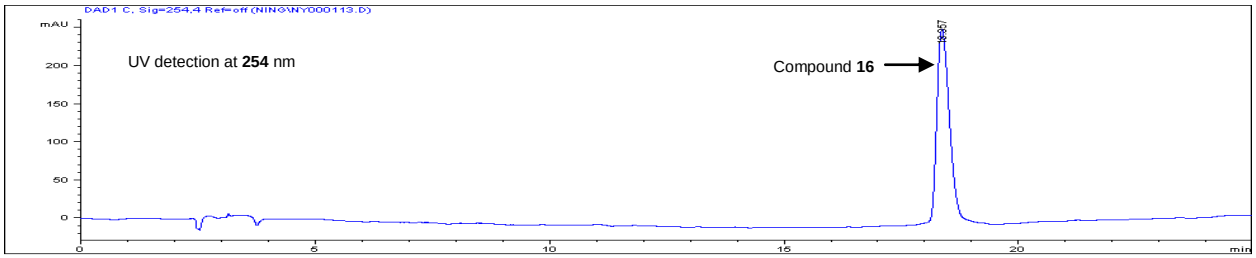

Figure **2.23**: Analytical HPLC profile of compound **16** after purification by preparative HPLC. Retention time = 18.3 min. Purity by HPLC > 99%.

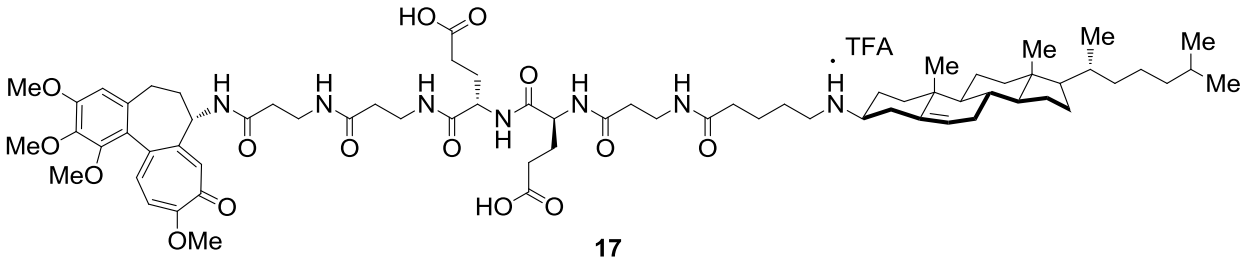

17

(S)-5-(((S)-4-carboxy-1-oxo-1-((3-oxo-3-((3-oxo-3-(((S)-1,2,3,10-tetramethoxy-9-oxo-5,6,7,9-tetrahydrobenzo[a]heptalen-7-yl)amino)propyl)amino)propyl)amino)butan-2-yl)amino)-4-(3-(5-(((3S,8S,9S,10R,13R,14S,17R)-10,13-dimethyl-17-((R)-6-methylheptan-2-yl)-2,3,4,7,8,9,10,11,12,13,14,15,16,17-tetradecahydro-1H-cyclopenta[a]phenanthren-3-yl)amino)pentanamido)propanamido)-5-oxopentanoic acid (17). 13 (9 mg, 0.025 mmol) was dissolved in anhydrous CH_2Cl_2 (1 mL). To a solution of **15** (35 mg, 0.03 mmol) were added HATU (14 mg, 0.037 mmol) and DIEA (13 mg, 0.1 mmol). After 30 min, the CH_2Cl_2 solution of deacetylcolchicine was added. The reaction was stirred for 16 h at 22 ^oC and then was concentrated *in vacuo*. The residue was dissolved in CH_2Cl_2 (5 mL) containing TFA (15%) and

stirred for 3 h at 22 ^{o}C. The reaction was concentrated *in vacuo,* and the crude product was purified by preparative reverse-phase HPLC (gradient: 89.95% H_2O, 9.95% MeCN, and 0.1 % TFA to 99.9% MeCN and 0.1% TFA over 20 min; retention time = 17.2 min (254 nm)), which afforded **17** (22 mg, 70%) as an off white solid. LRMS (ESI-) *m/z* 1296.8 ($M+H^-$, $C_{71}H_{105}N_7O_{15}$ requires 1296.8).

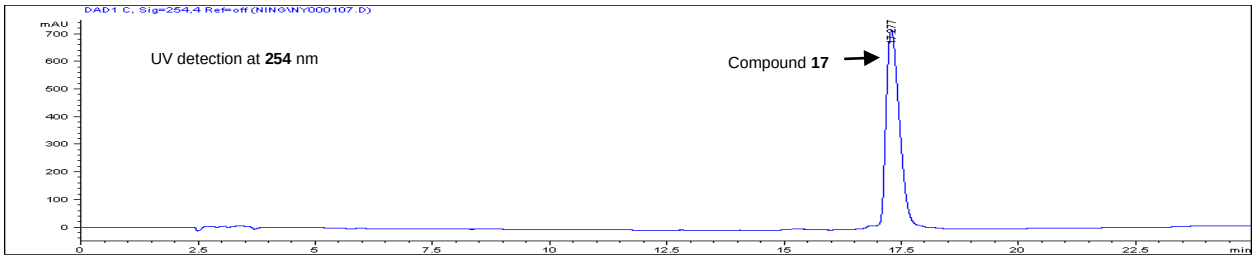

Figure **2.24**: Analytical HPLC profile of compound **17** after purification by preparative HPLC. Retention time = 17.2 min. Purity by HPLC > 99%.

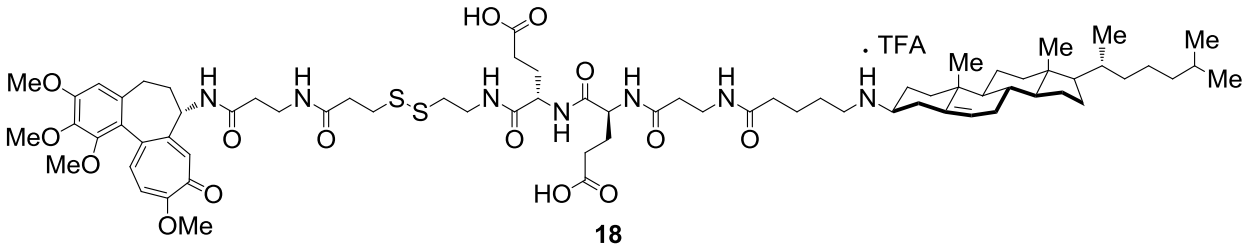

18

(14S,17S)-14-(2-carboxyethyl)-17-(3-(5-(((3S,8S,9S,10R,13R,14S,17R)-10,13-dimethyl-17-((R)-6-methylheptan-2-yl)-2,3,4,7,8,9,10,11,12,13,14,15,16,17-tetradecahydro-1H-cyclopenta[a]phenanthren-3-yl)amino)pentanamido)propanamido)-1,5,13,16-tetraoxo-1-(((S)-1,2,3,10-tetramethoxy-9-oxo-5,6,7,9-tetrahydrobenzo[a]heptalen-7-yl)amino)-8,9-dithia-4,12,15-triazaicosan-20-oic acid (18). 13 (12 mg, 0.034 mmol) was dissolved in anhydrous CH_2Cl_2 (2 mL). To a solution of Fmoc-β-Ala-OH (13 mg, 0.041 mmol) were added HATU (19 mg, 0.051 mmol) and DIEA (13 mg, 0.14 mmol). After 30 min, the CH_2Cl_2 solution of deacetylcolchicine was added. The reaction was stirred for 16 h at 22 ^{o}C. This solution was

diluted with CH_2Cl_2 (10 mL) and washed with aqueous NaOH (0.1 M, 5 mL) and saturated aqueous NaCl (5 mL). The organic layer was dried over anhydrous Na_2SO_4 and concentrated *in vacuo*. The residue was dissolved in DMF (2 mL) and to this solution were added silica-bound piperazine (1.07 mmol/g, 0.17 mmol, 158 mg) and DIEA (22 mg, 0.17 mmol). The reaction was stirred for 16 h at 22 ^oC. Silica-bound piperazine was removed by filtration and washed with CH_2Cl_2 (3×2 mL). The filtrates were concentrated *in vacuo* and the derived primary amine (deacetylcolchicine-β-Ala-NH_2) was dissolved in CH_2Cl_2 (1 mL). To a solution of **14** (40 mg, 0.034 mmol) were added HATU (19 mg, 0.051 mmol) and DIEA (13 mg, 0.14 mmol). After 30 min, the CH_2Cl_2 solution of the primary amine was added. The reaction was stirred for 16 h at 22 ^oC and then was concentrated *in vacuo.* The residue was dissolved in CH_2Cl_2 (5 mL) containing TFA (15%) and stirred for 3 h at 22 ^oC. The reaction was concentrated *in vacuo,* and the crude product was purified by preparative reverse-phase HPLC (gradient: 89.95% H_2O, 9.95% MeCN, and 0.1 % TFA to 99.9% MeCN and 0.1% TFA over 20 min; retention time = 17.8 min (254 nm)), which afforded **18** (7 mg, 15%) as a white solid. LRMS (ESI-) *m/z* 1388.5 ($M-H^-$, $C_{73}H_{108}N_7O_{15}S_2$ requires 1388.8).

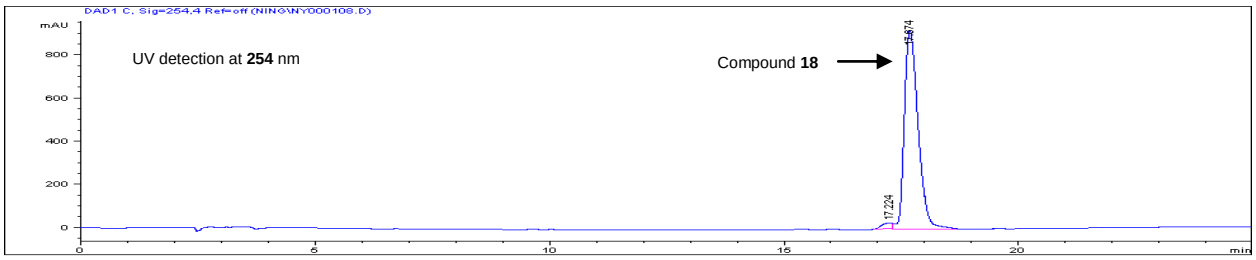

Figure **2.25**: Analytical HPLC profile of compound **18** after purification by preparative HPLC. Retention time = 17.8 min. Purity by HPLC > 95%.

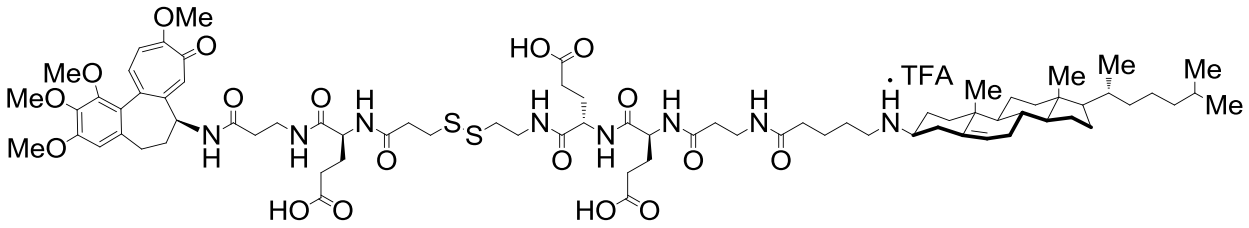

19

(4S,15S,18S)-15-(2-carboxyethyl)-18-(3-(5-(((3S,8S,9S,10R,13R,14S,17R)-10,13-dimethyl-17-((R)-6-methylheptan-2-yl)-2,3,4,7,8,9,10,11,12,13,14,15,16,17-tetradecahydro-1H-cyclopenta[a]phenanthren-3-yl)amino)pentanamido)propanamido)-6,14,17-trioxo-4-((3-oxo-3-(((S)-1,2,3,10-tetramethoxy-9-oxo-5,6,7,9-tetrahydrobenzo[a]heptalen-7-yl)amino)propyl)carbamoyl)-9,10-dithia-5,13,16-triazahenicosane-1,21-dioic acid (19). A side-chain protected dipeptide sequence (Fmoc-Glu(t-Bu)-β-Ala-OH) was synthesized on 2-Chlorotrityl resin (1.04 mmol/g, 96 mg, 0.1 mmol) using the method described for preparation of peptide **14**. Using this dipeptide (20 mg, 0.04 mmol) instead of Fmoc-β-Ala-OH, the primary amine (deacetylcolchicine-β-Ala-Glu(t-Bu)-NH_2) was synthesized with the same method for preparation of deacetylcolchicine-β-Ala-NH_2. The primary amine was dissolved in CH_2Cl_2 (1 mL). To a solution of **14** (40 mg, 0.034 mmol) were added HATU (19 mg, 0.051 mmol) and DIEA (18 mg, 0.14 mmol). After 30 min, the CH_2Cl_2 solution of the primary amine was added. The reaction was stirred for 16 h at 22 ^oC and then was concentrated *in vacuo.* The residue was dissolved in CH_2Cl_2 (5 mL) containing TFA (15%) and stirred for 3 h at 22 ^oC. The reaction was concentrated *in vacuo,* and the crude product was purified by preparative reverse-phase HPLC (gradient: 89.95% H_2O, 9.95% MeCN, and 0.1 % TFA to 99.9% MeCN and 0.1% TFA over 20 min; retention time = 17.1 min (254 nm)), which afforded **19** (9 mg, 17%) as a white solid. LRMS (ESI-) *m/z* 1515.4 ($M-H^-$, $C_{78}H_{116}N_8O_{18}S_2$ requires 1515.8).

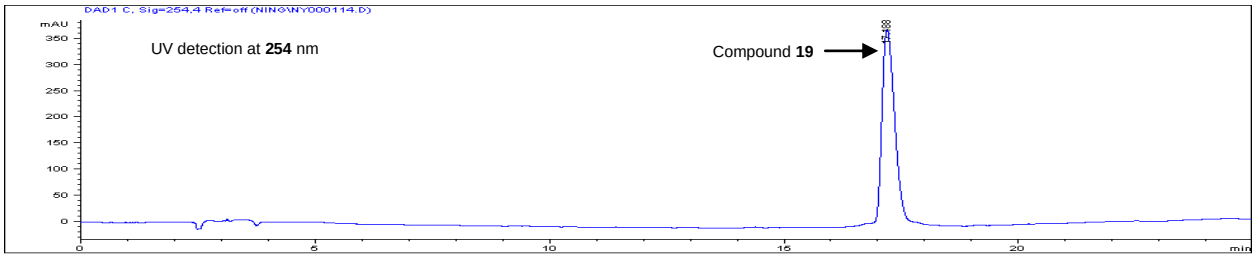

Figure **2.26**: Analytical HPLC profile of compound **19** after purification by preparative HPLC. Retention time = 17.1 min. Purity by HPLC > 99%.

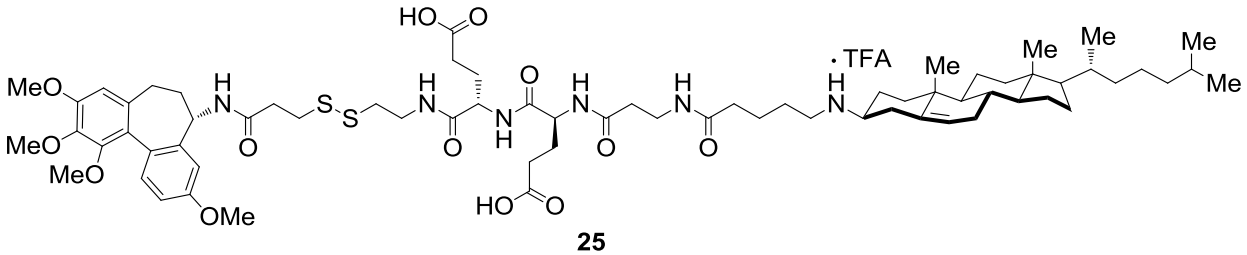

25

(4S)-5-(((2S)-4-carboxy-1-oxo-1-((2-((3-oxo-3-(((5S)-3,9,10,11-tetramethoxy-6,7-dihydro-5H-dibenzo[a,c][7]annulen-5-yl)amino)propyl)disulfanyl)ethyl)amino)butan-2-yl)amino)-4-(3-(5-(((3S,8S,9S,10R,13R,14S,17R)-10,13-dimethyl-17-((R)-6-methylheptan-2-yl)-2,3,4,7,8,9,10,11,12,13,14,15,16,17-tetradecahydro-1H-cyclopenta[a]phenanthren-3-yl)amino)pentanamido)propanamido)-5-oxopentanoic acid (25). 24 (11 mg, 0.03 mmol) was dissolved in anhydrous CH_2Cl_2 (1 mL). To a solution of **14** (43 mg, 0.036 mmol) were added EDC (8.6 mg, 0.045 mmol) and HOBt (6.9 mg, 0.045 mmol). After 30 min, the CH_2Cl_2 solution of deacetylcolchinol methyl ether was added. The reaction was stirred for 16 h at 22 ^oC and then was concentrated *in vacuo*. The residue was dissolved in CH_2Cl_2 (5 mL) containing TFA (15%) and stirred for 3 h at 22 ^oC. The reaction was concentrated *in vacuo,* and the crude product was purified by preparative reverse-phase HPLC (gradient: 89.95% H_2O, 9.95% MeCN, and 0.1 % TFA to 99.9% MeCN and 0.1% TFA over 20 min; retention time = 19.9 min (254 nm)), which afforded **25** (21 mg, 55%) as a white solid. LRMS (ESI-) *m/z* 1289.6 ($M+H^-$, $C_{69}H_{104}N_6O_{13}S_2$ requires 1289.7).

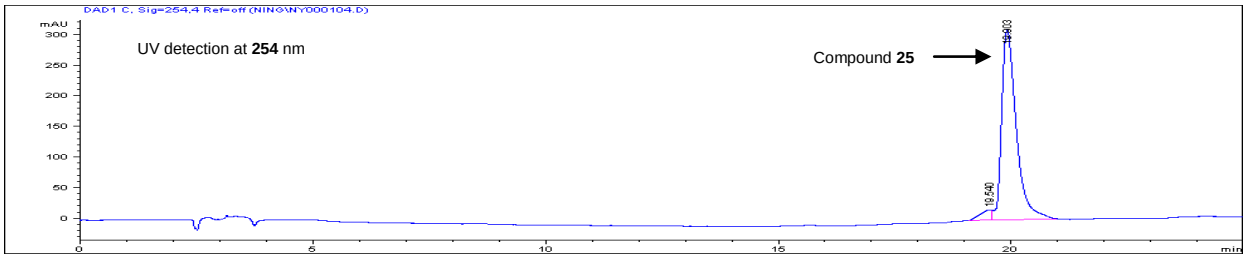

Figure **2.27**: Analytical HPLC profile of compound **25** after purification by preparative HPLC. Retention time = 19.9 min. Purity by HPLC > 95%.

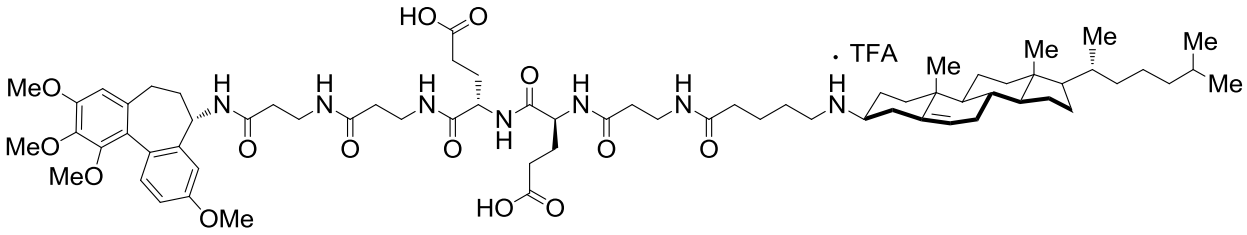

26

(4S)-5-(((2S)-4-carboxy-1-oxo-1-((3-oxo-3-((3-oxo-3-(((5S)-3,9,10,11-tetramethoxy-6,7-dihydro-5H-dibenzo[a,c][7]annulen-5-yl)amino)propyl)amino)propyl)amino)butan-2-yl)amino)-4-(3-(5-(((3S,8S,9S,10R,13R,14S,17R)-10,13-dimethyl-17-((R)-6-methylheptan-2-yl)-2,3,4,7,8,9,10,11,12,13,14,15,16,17-tetradecahydro-1H-cyclopenta[a]phenanthren-3-yl)amino)pentanamido)propanamido)-5-oxopentanoic acid (26). 24 (11 mg, 0.03 mmol) was dissolved in anhydrous CH_2Cl_2 (1 mL). To a solution of **15** (42 mg, 0.036 mmol) were added EDC (8.6 mg, 0.045 mmol) and HOBt (6.9 mg, 0.045 mmol). After 30 min, the CH_2Cl_2 solution of deacetylcolchinol methyl ether was added. The reaction was stirred for 16 h at 22 ^oC and then was concentrated *in vacuo*. The residue was dissolved in CH_2Cl_2 (5 mL) containing TFA (15%) and stirred for 3 h at 22 ^oC. The reaction was concentrated *in vacuo,* and the crude product was purified by preparative reverse-phase HPLC (gradient: 89.95% H_2O, 9.95% MeCN, and 0.1 % TFA to 99.9% MeCN and 0.1% TFA over 20 min; retention time = 18.6 min (254 nm)), which afforded **26** (25 mg, 67%) as a white solid. LRMS (ESI-) *m/z* 1268.8 ($M+H^-$, $C_{71}H_{105}N_7O_{15}$ requires 1268.8).

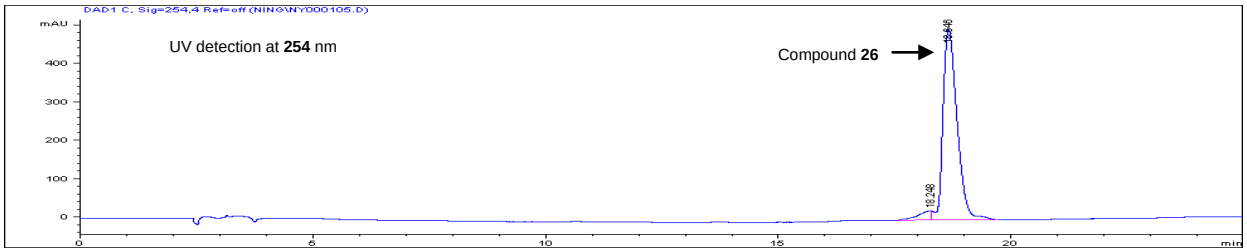

Figure **2.28**: Analytical HPLC profile of compound **26** after purification by preparative HPLC. Retention time = 18.6 min. Purity by HPLC > 95%.

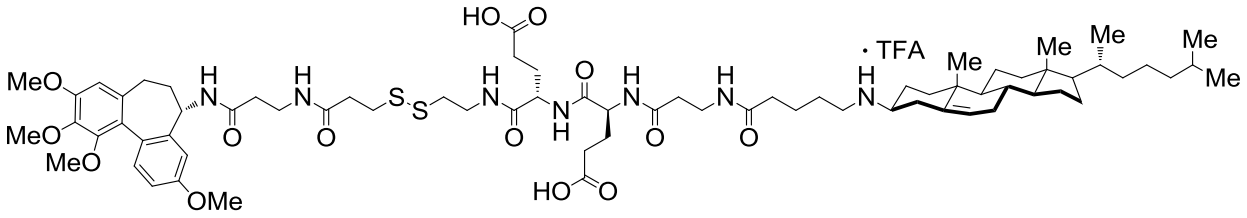

27

(14S,17S)-14-(2-carboxyethyl)-17-(3-(5-(((3S,8S,9S,10R,13R,14S,17R)-10,13-dimethyl-17-((R)-6-methylheptan-2-yl)-2,3,4,7,8,9,10,11,12,13,14,15,16,17-tetradecahydro-1H-cyclopenta[a]phenanthren-3-yl)amino)pentanamido)propanamido)-1,5,13,16-tetraoxo-1-(((5S)-3,9,10,11-tetramethoxy-6,7-dihydro-5H-dibenzo[a,c][7]annulen-5-yl)amino)-8,9-dithia-4,12,15-triazaicosan-20-oic acid (27). 24 (14 mg, 0.038 mmol) was dissolved in anhydrous CH_2Cl_2 (2 mL). To a solution of Fmoc-β-Ala-OH (14 mg, 0.045 mmol) were added EDC (10.9 mg, 0.057 mmol) and HOBt (8.7 mg, 0.057 mmol). After 30 min, the CH_2Cl_2 solution of deacetylcolchinol methyl ether was added. The reaction was stirred for 16 h at 22 ^oC. This solution was diluted with CH_2Cl_2 (10 mL) and washed with aqueous NaOH (0.1 M, 5 mL) and saturated aqueous NaCl (5 mL). The organic layer was dried over anhydrous Na_2SO_4 and concentrated *in vacuo*. The residue was dissolved in DMF (2 mL) and to this solution were added silica-bound piperazine (1.07 mmol/g, 0.19 mmol, 178 mg) and DIEA (24 mg, 0.19 mmol). The reaction was stirred for 16 h at 22 ^oC. Silica-bound piperazine was removed by filtration and washed with CH_2Cl_2 (3×2 mL). The filtrates were concentrated *in vacuo* and the derived primary amine (Deacetylcolchicine-β-Ala-NH_2) was dissolved in CH_2Cl_2 (1 mL). To a

solution of **14** (45 mg, 0.038 mmol) were added HATU (22 mg, 0.057 mmol) and DIEA (24 mg, 0.19 mmol). After 30 min, the CH_2Cl_2 solution of the primary amine was added. The reaction was stirred for 16 h at 22 ^oC and then was concentrated *in vacuo.* The residue was dissolved in CH_2Cl_2 (5 mL) containing TFA (15%) and stirred for 3 h at 22 ^oC. The reaction was concentrated *in vacuo,* and the crude product was purified by preparative reverse-phase HPLC (gradient: 89.95% H_2O, 9.95% MeCN, and 0.1 % TFA to 99.9% MeCN and 0.1% TFA over 20 min; retention time = 18.5 min (254 nm)), which afforded **27** (10 mg, 20%) as a white solid. LRMS (ESI-) *m/z* 1360.6 ($M+H^-$, $C_{73}H_{108}N_7O_{15}S_2$ requires 1360.7).

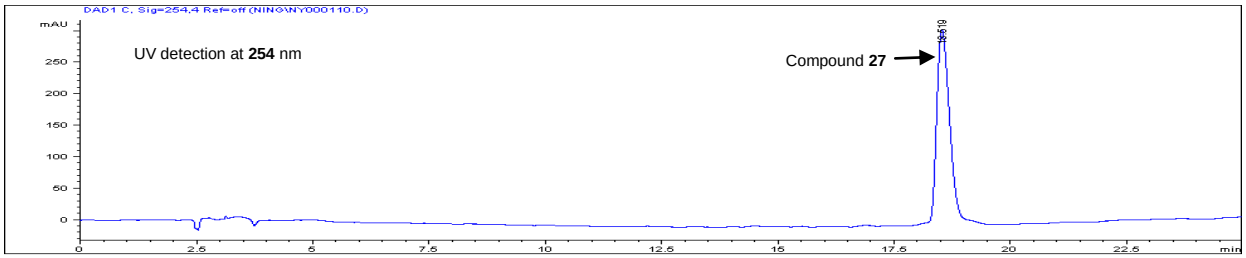

Figure **2.29**: Analytical HPLC profile of compound **27** after purification by preparative HPLC. Retention time = 18.5 min. Purity by HPLC > 99%.

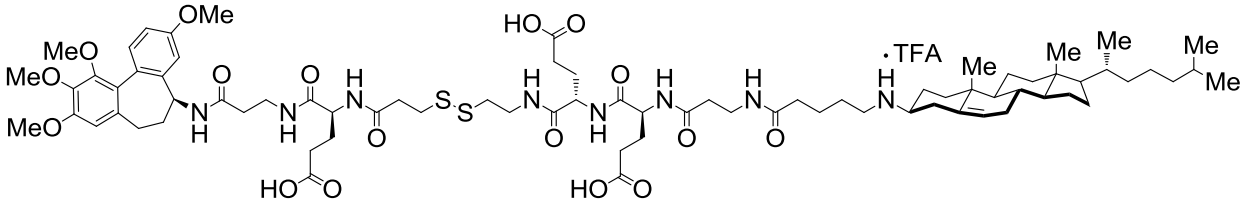

28

(4S,15S,18S)-15-(2-carboxyethyl)-18-(3-(5-(((3S,8S,9S,10R,13R,14S,17R)-10,13-dimethyl-17-((R)-6-methylheptan-2-yl)-2,3,4,7,8,9,10,11,12,13,14,15,16,17-tetradecahydro-1H-cyclopenta[a]phenanthren-3-yl)amino)pentanamido)propanamido)-6,14,17-trioxo-4-((3-oxo-3-(((5S)-3,9,10,11-tetramethoxy-6,7-dihydro-5H-dibenzo[a,c][7]annulen-5-yl)amino)propyl)carbamoyl)-9,10-dithia-5,13,16-triazahenicosane-1,21-dioic acid (28). A primary amine (deacetylcolchinol methyl ether-β-Ala-Glu(t-Bu)-NH_2) was synthesized with the

same method for preparation of deacetylcolchicine-β-Ala-Glu(t-Bu)-NH_2using deacetylcolchinol methyl ether hydrochloride instead of deacetylcolchicine. The primary amine (15 mg, 0.025 mmol) was dissolved in CH_2Cl_2 (1 mL). To a solution of **14** (36 mg, 0.03 mmol) were added HATU (14 mg, 0.038 mmol) and DIEA (13 mg, 0.1 mmol). After 30 min, the CH_2Cl_2 solution of the primary amine was added. The reaction was stirred for 16 h at 22 ^oC and then was concentrated *in vacuo.* The residue was dissolved in CH_2Cl_2 (5 mL) containing TFA (15%) and stirred for 3 h at 22 ^oC. The reaction was concentrated *in vacuo,* and the crude product was purified by preparative reverse-phase HPLC (gradient: 89.95% H_2O, 9.95% MeCN, and 0.1 % TFA to 99.9% MeCN and 0.1% TFA over 20 min; retention time = 18.1 min (254 nm)), which afforded **28** (7 mg, 19%) as a white solid. LRMS (ESI-) *m/z* 1489.9 ($M+H^-$, $C_{77}H_{116}N_8O_{17}S_2$ requires 1489.8).

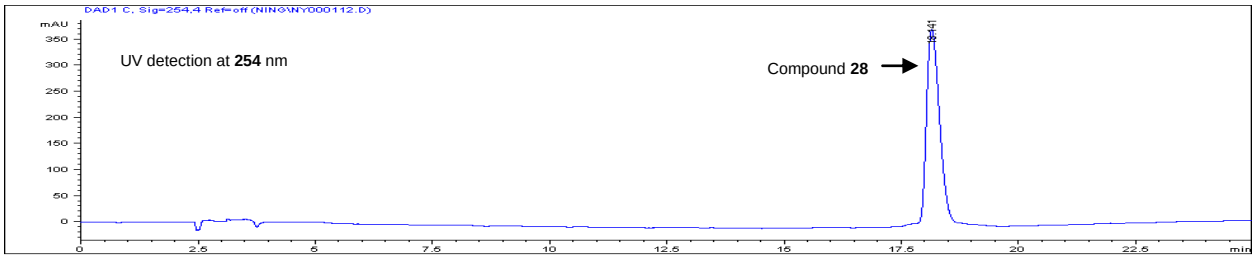

Figure **2.30**: Analytical HPLC profile of compound **28** after purification by preparative HPLC. Retention time = 18.1 min. Purity by HPLC > 99%.

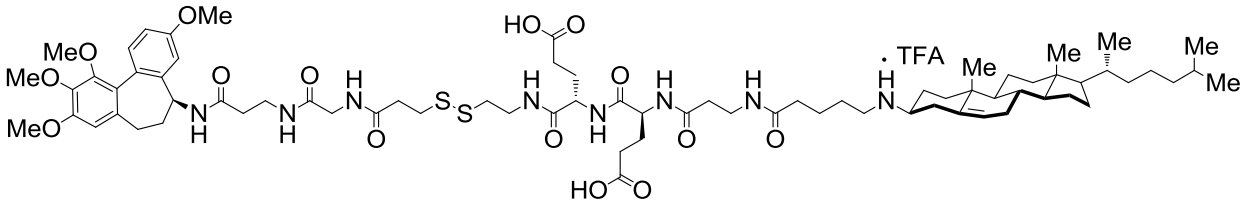

29

(17S,20S)-17-(2-carboxyethyl)-20-(3-(5-(((3S,8S,9S,10R,13R,14S,17R)-10,13-dimethyl-17-((R)-6-methylheptan-2-yl)-2,3,4,7,8,9,10,11,12,13,14,15,16,17-tetradecahydro-1H-cyclopenta[a]phenanthren-3-yl)amino)pentanamido)propanamido)-1,5,8,16,19-pentaoxo-

1-(((5S)-3,9,10,11-tetramethoxy-6,7-dihydro-5H-dibenzo[a,c][7]annulen-5-yl)amino)-11,12-dithia-4,7,15,18-tetraazatricosan-23-oic acid (29). A dipeptide sequence (Fmoc-Gly-β-Ala-OH) was conducted on 2-Chlorotrityl resin (1.04 mmol/g, 96 mg, 0.1 mmol) using the method described for preparation of peptide **14**. Using this dipeptide (14 mg, 0.04 mmol) instead of Fmoc-β-Ala-OH, the primary amine (deacetylcolchinol methyl ether-β-Ala-Gly-NH_2) was synthesized with the same method for preparation of deacetylcolchinol methyl ether-β-Ala-NH_2. The primary amine (11 mg, 0.025 mmol) was dissolved in CH_2Cl_2 (1 mL). To a solution of **14** (36 mg, 0.03 mmol) were added HATU (14 mg, 0.038 mmol) and DIEA (13 mg, 0.1 mmol). After 30 min, the CH_2Cl_2 solution of the primary amine was added. The reaction was stirred for 16 h at 22 ^oC and then was concentrated *in vacuo.* The residue was dissolved in CH_2Cl_2 (5 mL) containing TFA (15%) and stirred for 3 h at 22 ^oC. The reaction was concentrated *in vacuo,* and the crude product was purified by preparative reverse-phase HPLC (gradient: 89.95% H_2O, 9.95% MeCN, and 0.1 % TFA to 99.9% MeCN and 0.1% TFA over 20 min; retention time = 18.2 min (254 nm)), which afforded **29** (8 mg, 23%) as a white solid. LRMS (ESI-) *m/z* 1417.7 ($M+H^-$, $C_{74}H_{112}N_8O_{15}S_2$ requires 1417.8).

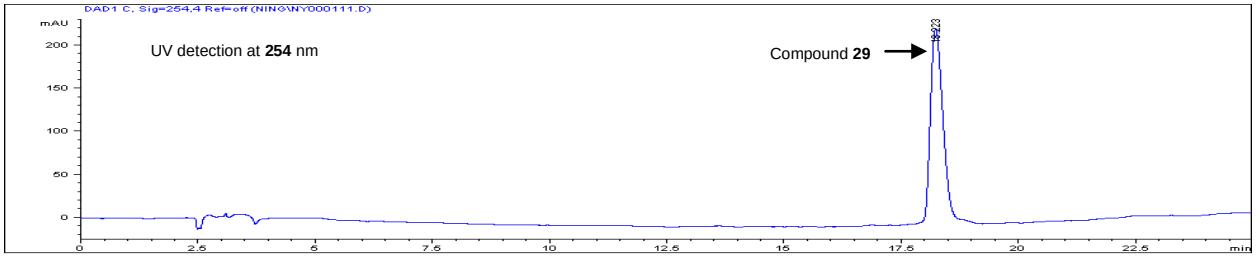

Figure **2.31**: Analytical HPLC profile of compound **29** after purification by preparative HPLC. Retention time = 18.2 min. Purity by HPLC > 99%.

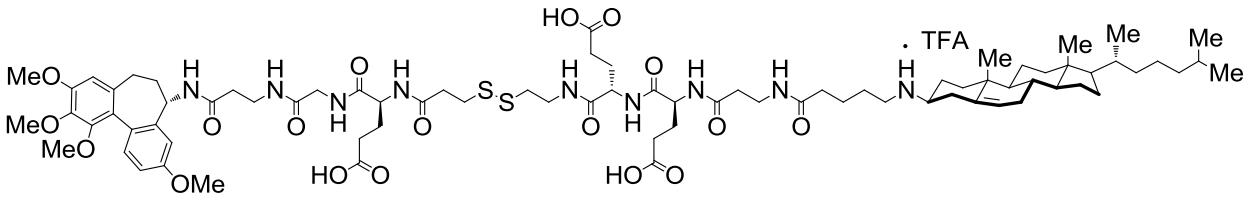

30

(4S,15S,18S)-15-(2-carboxyethyl)-18-(3-(5-(((3S,8S,9S,10R,13R,14S,17R)-10,13-dimethyl-17-((R)-6-methylheptan-2-yl)-2,3,4,7,8,9,10,11,12,13,14,15,16,17-tetradecahydro-1H-cyclopenta[a]phenanthren-3-yl)amino)pentanamido)propanamido)-6,14,17-trioxo-4-((2-oxo-2-((3-oxo-3-(((5S)-3,9,10,11-tetramethoxy-6,7-dihydro-5H-dibenzo[a,c][7]annulen-5-yl)amino)propyl)amino)ethyl)carbamoyl)-9,10-dithia-5,13,16-triazahenicosane-1,21-dioic acid (30). A side-chain protected tripeptide sequence (Fmoc-Glu(t-Bu)-Gly-β-Ala-OH) was conducted on 2-Chlorotrityl resin (1.04 mmol/g, 96 mg, 0.1 mmol) using the method described for preparation of peptide **14**. Using this tripeptide (22 mg, 0.04 mmol) instead of Fmoc-β-Ala-OH, the primary amine (deacetylcolchinol methyl ether-β-Ala-Gly-Glu(t-Bu)-NH_2) was synthesized with the same method for preparation of deacetylcolchinol methyl ether-β-Ala-NH_2. The primary amine (16 mg, 0.025 mmol) was dissolved in CH_2Cl_2 (1 mL). To a solution of **14** (36 mg, 0.03 mmol) were added HATU (14 mg, 0.038 mmol) and DIEA (13 mg, 0.1 mmol). After 30 min, the CH_2Cl_2 solution of the primary amine was added. The reaction was stirred for 16 h at 22 ^oC and then was concentrated *in vacuo.* The residue was dissolved in CH_2Cl_2 (5 mL) containing TFA (15%) and stirred for 3 h at 22 ^oC. The reaction was concentrated *in vacuo,* and the crude product was purified by preparative reverse-phase HPLC (gradient: 89.95% H_2O, 9.95% MeCN, and 0.1 % TFA to 99.9% MeCN and 0.1% TFA over 20 min; retention time = 17.9 min (254 nm)), which afforded **30** (10 mg, 26%) as a white solid. LRMS (ESI-) *m/z* 1546.9 ($M+H^-$, $C_{79}H_{119}N_9O_{18}S_2$ requires 1546.8).

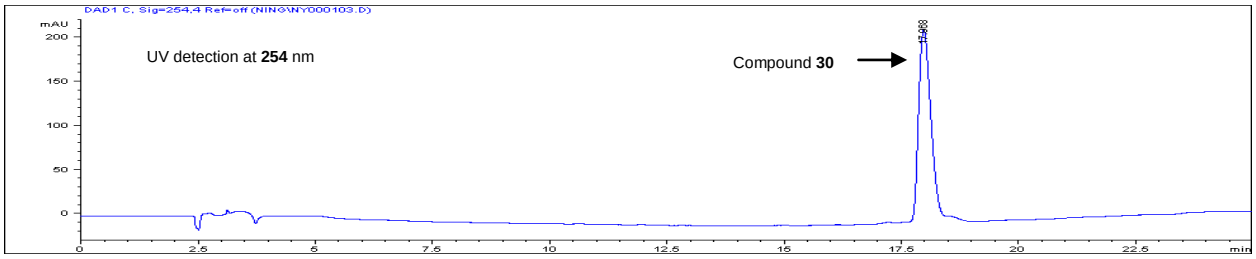

Figure **2.32**: Analytical HPLC profile of compound **30** after purification by preparative HPLC. Retention time = 17.9 min. Purity by HPLC > 99%.

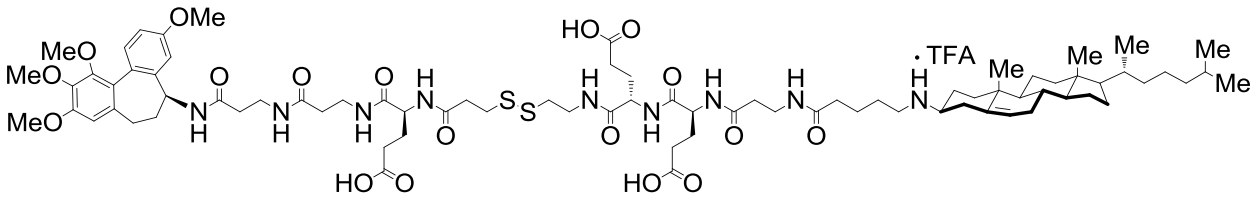

31

(4S,15S,18S)-15-(2-carboxyethyl)-18-(3-(5-(((3S,8S,9S,10R,13R,14S,17R)-10,13-dimethyl-17-((R)-6-methylheptan-2-yl)-2,3,4,7,8,9,10,11,12,13,14,15,16,17-tetradecahydro-1H-cyclopenta[a]phenanthren-3-yl)amino)pentanamido)propanamido)-6,14,17-trioxo-4-((3-oxo-3-((3-oxo-3-(((5R)-3,9,10,11-tetramethoxy-6,7-dihydro-5H-dibenzo[a,c][7]annulen-5-yl)amino)propyl)amino)propyl)carbamoyl)-9,10-dithia-5,13,16-triazahenicosane-1,21-dioic acid (31). A side-chain protected tripeptide sequence (Fmoc-Glu(t-Bu)-β-Ala-β-Ala-OH) was conducted on 2-Chlorotrityl resin (1.04 mmol/g, 96 mg, 0.1 mmol) using the method described for preparation of peptide **14**. Using this tripeptide (22 mg, 0.04 mmol) instead of Fmoc-β-Ala-OH, the primary amine (deacetylcolchinol methyl ether-β-Ala-β-Ala-Glu(t-Bu)-NH_2) was synthesized with the same method for preparation of deacetylcolchinol methyl ether-β-Ala-NH_2. The primary amine (16 mg, 0.025 mmol) was dissolved in CH_2Cl_2 (1 mL). To a solution of **14** (36 mg, 0.03 mmol) were added HATU (14 mg, 0.038 mmol) and DIEA (13 mg, 0.1 mmol). After 30 min, the CH_2Cl_2 solution of the primary amine was added. The reaction was stirred for 16 h at 22 ^oC and then was concentrated *in vacuo.* The residue was dissolved in CH_2Cl_2 (5 mL) containing

TFA (15%) and stirred for 3 h at 22 ^{o}C. The reaction was concentrated *in vacuo,* and the crude product was purified by preparative reverse-phase HPLC (gradient: 89.95% H_2O, 9.95% MeCN, and 0.1 % TFA to 99.9% MeCN and 0.1% TFA over 20 min; retention time = 17.9 min (254 nm)), which afforded **31** (8 mg, 21%) as a white solid. LRMS (ESI-) *m/z* 1560.8 ($M-H^-$, $C_{80}H_{121}N_9O_{18}S_2$ requires 1560.8).

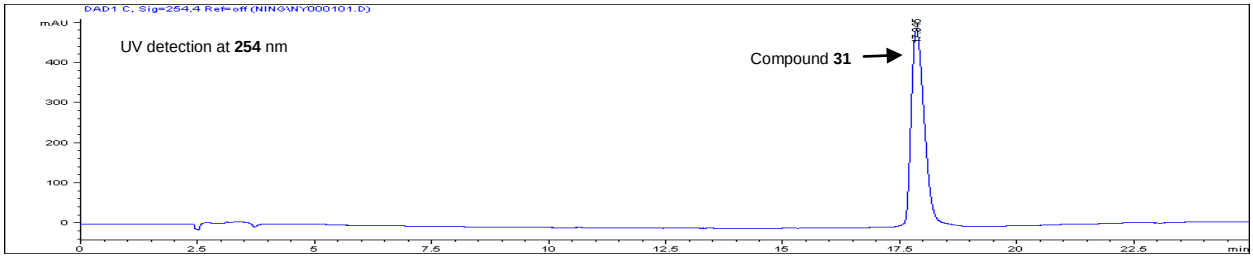

Figure **2.33**: Analytical HPLC profile of compound **31** after purification by preparative HPLC. Retention time = 17.9 min. Purity by HPLC > 99%.

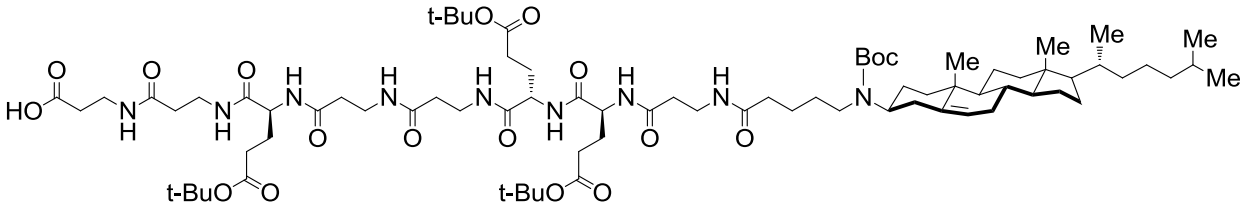

32

(16S,19S,30S)-16,19,30-tris(3-(tert-butoxy)-3-oxopropyl)-5-((3S,8S,9S,10R,13R,14S,17R)-10,13-dimethyl-17-((R)-6-methylheptan-2-yl)-2,3,4,7,8,9,10,11,12,13,14,15,16,17-tetradecahydro-1H-cyclopenta[a]phenanthren-3-yl)-2,2-dimethyl-4,10,14,17,20,24,28,31,35-nonaoxo-3-oxa-5,11,15,18,21,25,29,32,36-nonaazanonatriacontan-39-oic acid (32). Peptide **32** was constructed on 2-Chlorotrityl resin (1.04 mmol/g, 96 mg, 0.1 mmol) using the method described for preparation of peptide **14**. After completing all the steps of coupling reactions, the product was cleaved from the resin with TFA/TFE/CH_2Cl_2 (1:2:7) by shaking for 2h and purified by preparative reverse-phase HPLC (gradient: 89.95% H_2O, 9.95% MeCN, and 0.1 % TFA to 99.9% MeCN and 0.1% TFA over 10

min; retention time = 20.0 min (214 nm)) to afford **32** as a white solid (55 mg, 37%). LRMS (ESI-) *m/z* 1497.2 ($M+H^-$, $C_{79}H_{133}N_9O_{18}$ requires 1496.0).

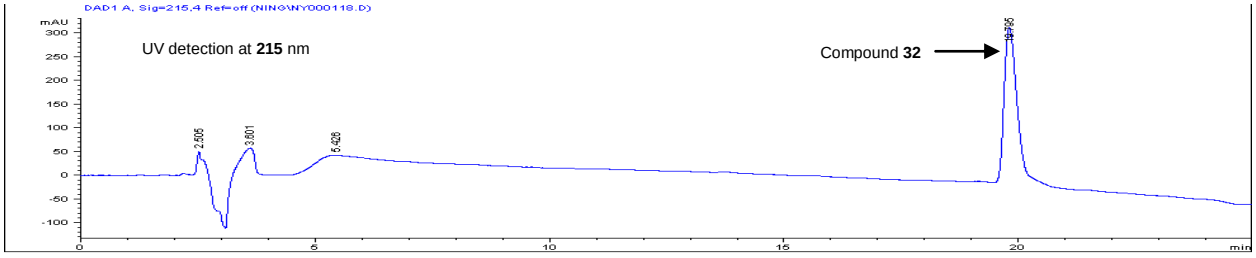

Figure **2.34**: Analytical HPLC profile of compound **32** after purification by preparative HPLC. Retention time = 20.0 min. Purity by HPLC > 99%.

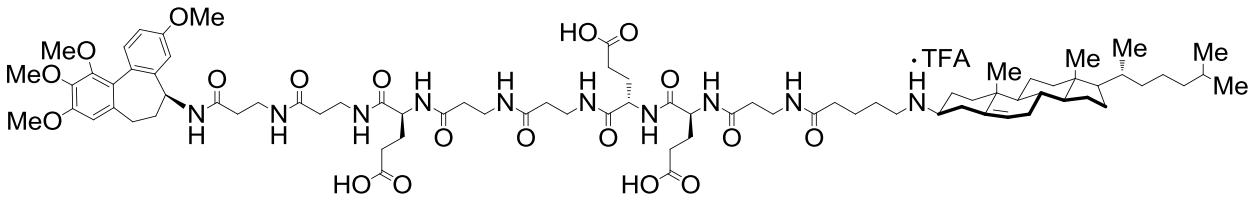

33

(4S,15S,18S)-15-(2-carboxyethyl)-18-(3-(5-(((3S,8S,9S,10R,13R,14S,17R)-10,13-dimethyl-17-((R)-6-methylheptan-2-yl)-2,3,4,7,8,9,10,11,12,13,14,15,16,17-tetradecahydro-1H-cyclopenta[a]phenanthren-3-yl)amino)pentanamido)propanamido)-6,10,14,17-tetraoxo-4-((3-oxo-3-((3-oxo-3-(((5R)-3,9,10,11-tetramethoxy-6,7-dihydro-5H-dibenzo[a,c][7]annulen-5-yl)amino)propyl)amino)propyl)carbamoyl)-5,9,13,16-tetraazahenicosane-1,21-dioic acid (33). 24 (11 mg, 0.03 mmol) was dissolved in anhydrous CH_2Cl_2 (1 mL). To a solution of **32** (54 mg, 0.036 mmol) were added EDC (8.6 mg, 0.045 mmol) and HOBt (6.9 mg, 0.045 mmol). After 30 min, the CH_2Cl_2 solution of deacetylcolchinol methyl ether was added. The reaction was stirred for 16 h at 22 ^oC and then was concentrated *in vacuo*. The residue was dissolved in CH_2Cl_2 (5 mL) containing TFA (15%) and stirred for 3 h at 22 ^oC. The reaction was concentrated *in vacuo,* and the crude product was purified by preparative reverse-phase HPLC (gradient: 89.95% H_2O, 9.95% MeCN, and 0.1 % TFA to 99.9% MeCN and 0.1% TFA over 20 min;

retention time = 17.0 min (254 nm)), which afforded **33** (10 mg, 22%) as a white solid. LRMS (ESI-) *m/z* 1539.9 ($M+H^-$, $C_{81}H_{122}N_{10}O_{19}$ requires 1539.9).

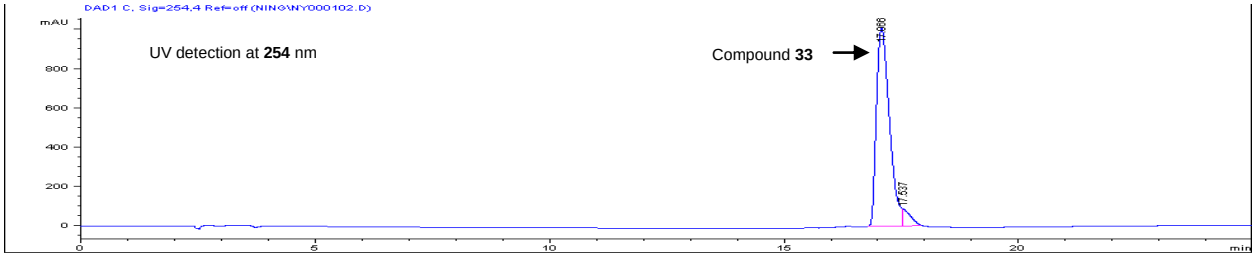

Figure **2.35**: Analytical HPLC profile of compound **33** after purification by preparative HPLC. Retention time = 17.0 min. Purity by HPLC > 95%.

2.5.3 Biological Assays and Protocols

Cell culture: Jurkat lymphocytes (human acute leukemia, ATCC #TIB-152) were cultivated in Roswell Park Memorial Institute (RPMI) 1640 medium supplemented with Fetal Bovine Serum (FBS, 10%), penicillin (100 units/mL), and streptomycin (100 µg/mL). PC-3 cells (Human prostate cancer cells, ATCC# CRL-1435) were cultivated in Dulbecco's Modified Eagle Medium/Nutrient Mixture F-12 (DMEM/F-12) medium supplemented with Fetal Bovine Serum (FBS, 10%), penicillin (100 units/mL), and streptomycin (100 µg/mL). DU-145 cells (Human prostate cancer cells, ATCC# HTB-81) were cultivated in RPMI 1640 medium supplemented with Fetal Bovine Serum (FBS, 10%), penicillin (100 units/mL), and streptomycin (100 µg/mL). A549 cells (Human lung adenocarcinoma epithelial cells, ATCC# CCL-185) were cultivated in F-12K 1640 medium supplemented with Fetal Bovine Serum (FBS, 10%), penicillin (100 units/mL), and streptomycin (100 µg/mL). All cell lines were propagated in a humidified 5% CO_2 incubator at 37 °C. Media used for cell culture and wash steps contained antibiotics and FBS unless otherwise noted.

Cell viability assay by flow cytometry

Jurkat lymphocytes (2.5×10^4) in media (250 µL) were loaded on a 96-well plate. To these cells, increasing concentrations of compounds (**10**, **23**, **16**-**19**, **25**-**31**, **33**) and compounds (**10**, **23**, **16**-**19**, **25**-**31**, **33**) with endosome disruptive peptide (**7** at 2 µM, **8** at 100 nM, or **9** at 1 µM) in DMSO (final [DMSO] = 0.8%) were added. After 48 h of incubation (72 h of incubation for **31**, **33** and **31**, **33** with **9** at 1 µM), propidium iodide was added to stain dead cells. Living cells were counted by flow cytometry.

PC3 cells (2.5×10^4) in media (250 µL) were loaded on a 96-well plate. After incubation for 24 h, the media was replaced with fresh media (250 µL) containing increasing concentrations of compounds (**23**, **31**, **33**) and compounds (**23**, **31**, **33**) with endosome disruptive peptide (1 µM **9**) in DMSO (final [DMSO] = 0.8%) were added. After 72 h of incubation, the cells in each well were washed with PBS (2 × 250 µL) and detached by treatment with a solution of trypsin (50 µL, 5 min). After detachment, fresh media (200 µL) was added to each well and propidium iodide was used to stain dead cells. Living cells were counted by flow cytometry.

DU145 cells (2.5×10^4) in media (250 µL) were loaded on a 96-well plate. After incubation for 24 h, the media was replaced with fresh media (250 µL) containing increasing concentrations of compounds (**23**, **31**, **33**) and compounds (**23**, **31**, **33**) with endosome disruptive peptide (1 µM **9**) in DMSO (final [DMSO] = 0.8%) were added. After 72 h of incubation, the cells in each well were washed with PBS (2 × 250 µL) and detached by treatment with a solution of trypsin (50 µL, 5 min). After detachment, fresh media (200 µL) was added to each well and propidium iodide was used to stain dead cells. Living cells were counted by flow cytometry.

A549 cells (2.5×10^4) in media (250 µL) were load on a 96-well plate. After incubation for 24 h, the media was replaced with fresh media (250 µL) containing increasing concentrations of compounds (**23**, **31**, **33**) and compounds (**23**, **31**, **33**) with endosome disruptive peptide (1 µM **9**) in DMSO (final [DMSO] = 0.8%) were added. After 72 h of incubation, the cells in each well were washed with PBS (2 × 250 µL) and detached by treatment with a solution of trypsin (50 µL,

5 min). After detachment, fresh media (200 µL) was added to each well and propidium iodide was used to stain dead cells. Living cells were counted by flow cytometry.

2.6 References

1. Allen, T. M.; Cullis, P. R. Drug delivery systems: entering the mainstream. *Science* **2004**, *303*, 1818-1822

2. Benjamin, L.; Quentin, J. B.; David, E. G. Protein therapeutics: a summary and pharmacological classification. *Nat. Rev. Drug Disc*. **2008**, *7*, 21-39.

3. Adams, G. P. Improving the tumor specificity and retention ofantibody-based molecules. *In Vivo*. **1998**, *12*, 11-21.

4. Pagnan, G.; Stuart, D. D.; Pastorino, F.; Raffaghello, L.; Montaldo, P. G.; Allen, T.; M. B. Calabretta, and Ponzoni, M. Delivery of c-myb antisense oligodeoxynucleotides to human neuroblastoma cells via disialoganglioside GD(2)-targeted immunoliposomes: antitumor effects. *J. Natl. Cancer Inst*. **2000**, *92*, 253-261.

5. Maruyama, K. In vivo targeting by liposomes. *Biol. Pharm. Bull*. **2000**, *23*, 791-799.

6. F. M. Muggia. Doxorubicin-polymer conjugates: further demonstration of the concept of enhanced permeability and retention. *Clin. Cancer Res*. **1999**, *5*, 7-8.

7. Lindgren, M.; Hallbrink, M.; Prochiantz, A.; Langel, U. Cell-penetrating peptides. *Trends Pharmacol*. *Sci*. **2000**, *21*, 99-103.

8. EI-Andaloussi, S.; Holm, T.; Langel, U. Cell-penetrating peptides: Mechanisms and applications. *Curr. Pharm. Des*. **2005**, *11*, 3597-3611.

9. Sudimack, J.; Lee, R. J. Targeted drug delivery via the folate receptor. *Adv. Drug Del. Rev*. **2000**, *41*, 147-162.

10. Vyas, S. P.; Singh, A.; Sihorkar, V. Ligand-receptor-mediated drug delivery: An emerging paradigm in cellular drug targeting. *Crit. Rev. Ther. Drug Carrier. Syst*. **2001**, *18*, 1-76.

11. Chung, N. S.; Wasan, K. M. Potential role of the low-density lipoprotein receptor family as mediators of cellular drug uptake. *Adv. Drug Del. Rev*. **2004**, *56*, 1315-1334.

12. Conner, S. D.; Schmid, S. L. Regulated portals of entry into the cell. *Nature* **2003**, *422*, 37-44.

13. Rudenko, G.; Henry, L.; Henderson, K.; Ichtchenko, K; Brown, M. S.; Goldstein, J. L. Deisenhofer, J. Structure of the LDL receptor extracellular domain at endosomal pH. *Science* **2002**, *298*, 2353-2358.

14. Jeon, H.; Blacklow, S. C. Structure and physiologic function of the low-density lipoprotein receptor. *Annu. Rev. Biochem*. **2005**, *74*, 535-562.

15. Maxfield, F. R.; McGraw, T. E. Endocytic recycling. *Nat. Rev. Mol. Cell Biol*. **2004**, *5*, 121-132.

16. Mesmin, B.; Maxfield, F. R. Intracellular sterol dynamics. *Biochim. Biophys. Acta* **2009**, *1791*, 636–645.

17. Hymel, D.; Peterson, B. R. Synthetic cell surface receptors for delivery of therapeutics and probes. *Adv. Drug Delivery Rev*. **2012**, *64*, 797-810.

18. Wolfrum, C.; Shi, S.; Jayaprakash, K. N.; Jayaraman, M.; Wang, G.; Pandey, R. K.; Rajeev, K. G.; Nakayama, T.; Charrise, K.; Ndungo, E. M.; Zimmermann, T.; Koteliansky, V.; Manoharan, M.; Stoffel, M. Mechanisms and optimization of *in vivo* delivery of lipophilic siRNAs. *Nat. Biotechnol*. **2007**, *25*, 1149-1157.

19. Pitard, B.; Oudrhiri, N.; Vigneron, J. P.; Hauchecorne, M.; Aguerre, O.; Toury, R.; Airiau, M.; Ramasawmy, R.; Scherman, D.; Crouzet, J.; Lehn, J. M.; Lehn, P. Structural characteristics of supramolecular assemblies formed by guanidinium-cholesterol reagents for gene transfection. *Proc. Natl. Acad. Sci. U.S.A.* **1999**, *96*, 2621-2626.

20. Sato, S. B.; Ishii, K.; Makino, A.; Iwabuchi, K.; Yamaji-Hasegawa, A.; Senoh, Y.; Nagaoka, I.; Sakuraba, H.; Kobayashi, T. Distribution and Transport of Cholesterol-rich Membrane

Domains Monitored by a Membrane-impermeant Fluorescent Polyethylene Glycol-derivatized Cholesterol. J. Biol. Chem. **2004**, *279*, 23790-23796.

21. Firestone, R. A. Low-Density Lipoprotein as a Vehicle for Targeting Antitumor Compounds to Cancer Cells. *Bioconjugate Chem*. **1994**, *5*, 105-113.

22. Kan, C. C.; Yan, J.; Bittman, R. Rates of spontaneous exchange of synthetic radiolabeled sterols between lipid vesicles. *Biochemistry* **1992**, *31*, 1866-1874.

23. Spencer, T. A.; Wang, P.; Li, D.; Russel, J. S.; Blank, D. H.; Huuskonen, J.; Fielding, P. E.; Fielding, C. J. Benzophenone-containing cholesterol surrogates: synthesis and biological evaluation. *J. Lipid Res*. **2004**, *45*, 1510-1518.

24. Salmi, C.; Loncle, C.; Vidal, N.; Laget, M.; Letourneux, Y.; Brunel, J. M. New 3-Aminosteroid Derivatives as a New Family of Topical Antibacterial Agents Active against Methicillin-Resistant Staphylococcus aureus (MRSA). Lett. Drug Des. Discovery **2008**, *5*, 169-172.

25. Peterson, B. R. Synthetic mimics of mammalian cell surface receptors: prosthetic molecules that augment living cells. *Org. Biomol. Chem*. **2005**, *3*, 3607-3612.

26. Lakadamyali, M.; Rust, M. J.; Zhuang, X. Endocytosis of influenza viruses. *Microbes Infect*. **2004**, *6*, 829-836.

27. Turk, M. J.; Reddy, J. A.; Chmielewski, J. A.; Low, P. S. Characterization of a novel pH-sensitive peptide that enhances drug release from folate-targeted liposomes at enhances drug release from folate-targeted liposomes at endosomal pHs. Biochim. Biophys. Acta **2002**, *1559*, 56-68.

28. Moore, N. M.; Sheppard C. L.; Barbour, T. R.; Sakiyama-Elbert, S.E. The effect of endosomal escape peptides on in vitro gene delivery of polyethylene glycol-based vehicles. *J Gene Med*. Published online: Jul 21, **2008**.

29. Wadia, J. S.; Stan, R. V.; Dowdy, S. F. Transducible TAT-HA fusogenic peptide enhances escape of TAT-fusion proteins after lipid raft macropinocytosis. *Nat. Med*. **2004**, *10*, 310-315.

30. Hirosue, S.; Weber, T. pH-Dependent lytic peptides discovered by phage display. *Biochemistry* **2006**, *45*, 6476-6487.

31. Austin, C. D.; Wen, X.; Gazzard, L.; Nelson, C.; Scheller, R. H.; Scales, S. J. Oxidizing potential of endosomes and lysosomes limits intracellular cleavage of disulfide-based antibody-drug conjugates. *Proc. Natl. Acad. Sci. USA* **2005**, *102*, 17987-17992.

32. Saito, G.; Swanson, J. A.; Lee, K. D. Drug delivery strategy utilizing conjugation via reversible disulfide linkages: role and site of cellular reducing activities. Adv. Drug Deliv. Rev. **2003**, *55*, 199-215.

33. Sun, Q.; Cai, S.; Peterson, B. R. Selective Disruption of Early/Recycling Endosomes: Release of Disulfide-Linked Cargo Mediated by a *N*-Alkyl-3β-Cholesterylamine-Capped Peptide. *J. Am. Chem. Soc*. **2008**, *130*, 10064-10065.

34. Horton, R. A.; Bagnator, J. D.; Grissom, C. B. Synthesis and characterization of a cobalamin-colchicine conjugate as a novel tumor-targeted cytotoxin. *J. Org. Chem*. **2004**, *69*, 8987-8996.

35. Boonyarattanakalin, S.; Martin, S. E.; Dykstra, S. A.; Peterson, B. R. Synthetic mimics of small mammalian cell surface receptors. *J. Am. Chem. Soc*. **2004**, *126*, 16379-16386.

36. Boonyarattanakalin, S.; Athavankar, S.; Sun, Q.; Peterson, B. R. Synthesis of an artificial cell surface receptor that enables oligohistidine affinity tags to function as metal-dependent cell-penetrating peptides. *J. Am. Chem. Soc.* **2006**, *128*, 386-387.

37. Kang, G. J.; Getahun, Z.; Muzaffar, A.; Brossi, A.; Hamel, E. *N*-acetylcolchinol *O*-methyl ether and thiocolchicine, potent analogues of colchicine modified in the C Ring. *J. Biol. Chem*. **1990**, *265*, 10255-10259.

38. Brossi, A.; Yeh, H. J.; Chrzanowska, M.; Wolff, J.; Hamel, E.; Lin, C. M.; Quinn, F.; Suffness, M.; Silverton, J. Colchicine and its analogues: recent findings. *Med. Res. Rev*. **1988**, *8*, 77-94.

39. Norman, N.; Jens, R.; Nikolay, S.; Janna, V.; Andreas, T.; Alexey, Y.; Hans, G. S. A convenient entry to new C-7-modified colchicinoids through azide alkyne [3+2] cycloaddition: application of ring-contractive rearrangements. *Heterocycles* **2011**, *82*, 1585-1600.

40. Gilbert, B.; Denis, B.; Indu, D.; Philip, K.; Eric, S.; Lik, R. T.; Thomas, B. A synthesis of (aR,7S)-(-)-N-acetylcolchinol and its conjugate with a cyclic RGD peptide. *Tetrahedron* **2008**, *64*, 4700-4710.

41. Tai, S.; Sun, Y.; Squires, J. M.; Zhang, H.; Oh, W. K.; Liang, C. Z.; Huang, J. PC3 is a cell line characteristic of prostatic small cell carcinoma. *Prostate* **2011**, *71*, 1668-1679.

42. Pulukuri, S. M.; Gondi, C. S.; Lakka, S. S. RNA interference-directed knockdown of urokinase plasminogen activator and urokinase plasminogen activator receptor inhibits prostate cancer cell invasion, survival, and tumorigenicity in vivo. *J. Biol. Chem*. **2005**, *280*, 36529-36540.

43. Lieber, M.; Smith, B.; Szakal, A.; Nelson-Rees, W.; Todaro, G. A continuous tumor-cell line from a human lung carcinoma with properties of type II alveolar epithelial cells. *Int. J. Cancer* **1976**, *17*, 62–70.

44. Weyel, D.; Sedlacek, H-H.; Muller, R.; Brusselbach, S. Secreted human β-glucuronidase: a novel tool for gene-directed enzyme prodrug therapy. *Gene Ther*. **2000**, *7*, 224-231.

45. Springer, C. J.; Niculescu-Duvaz, I. Prodrug-activating systems in suicide gene therapy. *J. Clin. Investig.* **2000**, *105*, 1161-1167.

46. Nenny, W. A.; Wilson, W. R. The design of selectively-activated anti-cancer prodrugs for use in antibody-directed and gene-directed enzyme-prodrug therapies. *J. Pharm. Pharmacol*. **1998**, *50*, 387-394.

47. Rautio J.; Kumpulainen, H.; Heimbach, T. Prodrugs: design and clinical applications. *Nat. Rev. Drug Discov*. **2008**, *7*, 255-270.

48. Egeblad, M.; Werb, Z. New functions for the matrix metalloproteinases in cancer progression. *Nat. Rev. Cancer* **2002**, *2*, 161-174.

49. Atkinson, J. M.; Falconer, R. A.; Edwards, D. R.; Pennington, C. J.; Siller, C. S.; Shnyder, S. D.; Bibby, M. C.; Patterson, L. H.; Loadman, P. M.; Gill, J. H. Development of a Novel Tumor-Targeted Vascular Disrupting Agent Activated by Membrane-Type Matrix Metalloproteinases. *Cancer Res*. **2010**, *70*, 6902-6912.

50. Victoria, V.; Ana R. S.; Mariano, R. H.; Aurore, D.; Ramkrishna, B.; Laura, C.; Gemma, M.; Hamdy A. R.; Isabel, B.; Robert, A.; Falconer, K. P. Synthesis and Biological Evaluation of Colchicine C-Ring Analogues Tethered with Aliphatic Linkers Suitable for Prodrug Derivatisation. *Bioorg. Med. Chem. Lett.* **2012**, *22*, 7693-7696.

51. Nimjee, S. M.; Rusconi, C. P.; Sullenger, B. A. Aptamers: an emerging class of therapeutics. *Annu. Rev. Med*. **2005**, *56*, 555-583.

52. Famulok, M. Oligonucleotide aptamers that recognize small molecules. Curr. Opin. Struct. Biol. **1999**, *9*, 324-329.

53. Morris, K. N.; Jensen, K. B.; Julin, C. M.; Weil, M.; Gold, L. High affinity ligands from in vitro selection: complex targets. *Proc. Natl. Acad. Sci. USA* **1998**, *95*, 2902-2907.

54. Chen, C. H.; Dellamaggiore, K. R.; Ouellette, C. P.; Sedano, C. D.; Lizadjohry, M.; Chernis, G.A.; Gonzales, M.; Baltasar, F. E.; Fan, A. L.; Myerowitz, R.; Neufeld, E. F.; Aptamer-based endocytosis of a lysosomal enzyme. *Proc. Natl. Acad. Sci. USA* **2008**, *105*, 15908-15913.

55. Levy-Nissenbaum, E.; Radovic-Moreno, A. F.; Wang, A. Z.; Langer, R.; Farokhzad, O. C. Nanotechnology and aptamers: Applications in drug delivery. Trends Biotechnol. **2008**, *26*, 442-449.

56. Rajasekaran, A. K.; Anilkumar, G.; Christiansen J. J. Is prostate-specific membrane antigen a multifunctional protein? *Am. J. Physiol. Cell Physiol*. **2005**, *288*, C975–981.

57. Ghosh, A.; Heston, W. D. Tumor target prostate specific membrane antigen (PSMA) and its regulation in prostate cancer. *J. Cell. Biochem*. **2004**, *91*, 528–539.

58. Sumith, A. K.; Zhigang, Z.; Jun, Y.; Carol, B. P.; Philip, S. L. Design, Synthesis, and Preclinical Evaluation of Prostate-Specific Membrane Antigen Targeted ^{99m}Tc-Radioimaging Agents. Mol. Pharm. **2009**, *6*, 790-800.